

NISTIR 5795

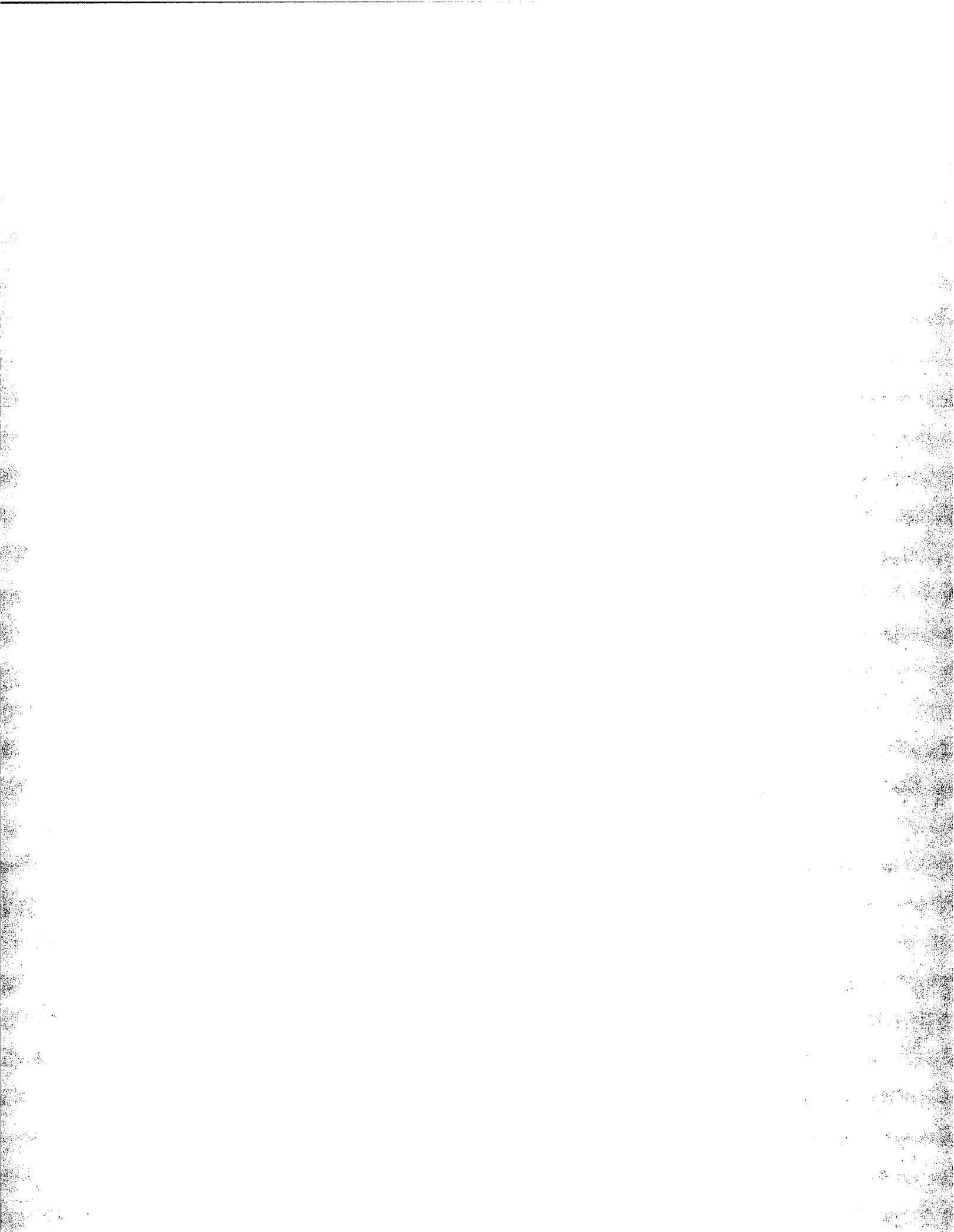
**Minimum Mass Flux Requirements to Suppress
Burning Surfaces with Water Sprays**

Jiann C. Yang
Charles I. Boyer
William L. Grosshandler

Building and Fire Research Laboratory
National Institute of Standards and Technology
Gaithersburg, MD 20899
April 1996



U.S. Department of Commerce
Michael Kantor, *Secretary*
Technology Administration
Mary L. Good, *Under Secretary for Technology*
National Institute of Standards and Technology
Arati Prabhakar, *Director*



CONTENTS

	Page
ACKNOWLEDGMENTS	v
ABSTRACT	vii
1. Introduction	1
2. Experimental Facility	3
2.1 Conical Heater	3
2.2 Heat Flux Gauge	3
2.3 Sample Holder, Sample Materials, and Load Cell	3
2.4 Droplet/Spray Generators	5
2.5 Water Flow System	8
2.6 Experimental Procedure	8
2.7 Experimental Conditions	9
3. Results and Discussion	9
3.1 Micronozzle Array Characterization	9
3.2 Piezoelectric Droplet Generator Characterization	9
3.3 Mass Burning Rates	12
3.4 Extinguishment Tests	13
3.4.1 Phenomenological Description of Flame Extinguishment Process	13
3.4.2 Micronozzle Array Results	15
3.4.3 Piezoelectric Droplet Generator Results	17
3.4.4 Surface Cooling by Water	22
4. Conclusions	24
5. Recommendations	25
6. References	25
Appendix A	27
Appendix B	29
Appendix C	32

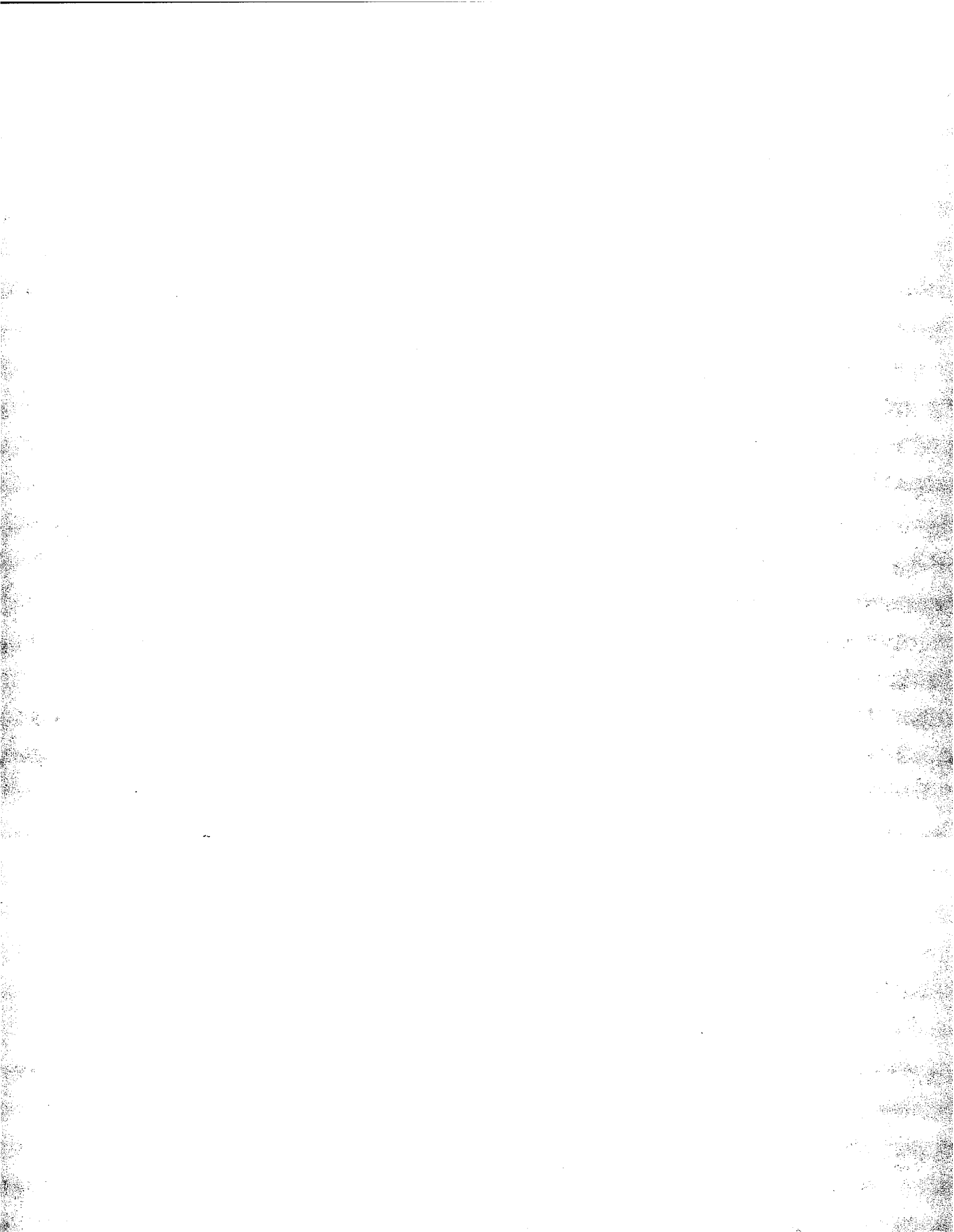
ACKNOWLEDGMENTS

This work was sponsored by the Federal Emergency Management Agency, United States Fire Administration. We would like to acknowledge the helpful guidance provided by Mr. Larry Maruskin of the U.S. Fire Administration, useful discussions with Professor Shi-Chune Yao of Carnegie Mellon University and Dr. Michael A. Delichatsios of the Factory Mutual Research Corporation, and the technical assistance of Messrs. Darren Lowe, Mike Glover, and William Rinkinen of BFRL/NIST and Dr. John Saylor formerly of, and Mr. Umar Khan of the Integrated Technology for Medicine (ITM), Inc. We would also like to thank Dr. Perry Skeath, President of ITM, for providing prototypes of micronozzle arrays used in some of the experiments reported herein. The work reported in **Appendix C** (as part of the overall FEMA sponsored water mist project) was performed by Mr. Anthony D. Putorti, Jr., Ms. Tamra D. Belsinger, and Mr. William H. Twilley under the supervision of Mr. Daniel Madrzykowski of the Fire Safety Engineering Division of BFRL. The authors would like to thank them for their effort.

ABSTRACT

Experimental measurements of extinguishment times of burning solid fuels using water were conducted using a prototype micronozzle array and a piezoelectric droplet generator. Solid fuels considered included solid white pine, polymethyl methacrylate, and polystyrene foam. External heat flux was applied to the sample surface during burning. The effects of drop size, sample orientation with respect to the nozzle, and nozzle distance from the sample surface on extinguishment time were examined. The extinguishment time was found to decrease with increasing water flow rate. For a given water flow rate, significant reduction in extinguishment time was observed when smaller droplets were used. At low water flow rates, the extinguishment time decreased when the nozzle was positioned further from the sample surface. At high flow rates, the extinguishment was independent of the nozzle-to-sample distance. When the droplet stream was 45° relative to the sample, the extinguishment time was not affected by the nozzle-to-sample distance.

The other component of the project was to evaluate a commercial low pressure, high momentum pendant water mist nozzle using an optical array probe droplet analyzer. The pendant nozzle used in this study is currently being evaluated by listing organizations for fire suppression in residential and light hazard occupancies. The objective of this study was to determine drop size and velocity distributions at various locations in the spray. Experiments were conducted at delivery pressures of $621 \text{ kPa} \pm 14 \text{ kPa}$ ($90.0 \text{ psi} \pm 2.0 \text{ psi}$) and $448 \text{ kPa} \pm 14 \text{ kPa}$ ($65.0 \text{ psi} \pm 2.0 \text{ psi}$). The droplet diameters from the experiments were found to range from less than $36 \mu\text{m}$ to $1230 \mu\text{m}$ for the experiments conducted at $448 \text{ kPa} \pm 14 \text{ kPa}$ ($65.0 \text{ psi} \pm 2.0 \text{ psi}$), and to range from less than $36 \mu\text{m}$ to $1155 \mu\text{m}$ for the experiments conducted at $621 \text{ kPa} \pm 14 \text{ kPa}$ ($90.0 \text{ psi} \pm 2.0 \text{ psi}$). The velocities of the water droplets were calculated based on the time required for each individual drop to pass through the probe image field. The range of droplet velocities was found to be approximately 0.19 m/s to 1.58 m/s (0.62 ft/s to 5.18 ft/s) from the experiments conducted at $448 \text{ kPa} \pm 14 \text{ kPa}$ ($65.0 \text{ psi} \pm 2.0 \text{ psi}$). For the measurements taken at $621 \text{ kPa} \pm 14 \text{ kPa}$ ($90.0 \text{ psi} \pm 2.0 \text{ psi}$), the droplet velocities ranged from approximately 0.25 m/s to 1.9 m/s (0.82 ft/s to 6.23 ft/s).



MINIMUM MASS FLUX REQUIREMENTS TO SUPPRESS BURNING SURFACES WITH WATER SPRAYS

Jiann C. Yang, Charles I. Boyer, and William L. Grosshandler
Building and Fire Research Laboratory

1. Introduction

Engineering correlations exist in the literature which allow a fire protection engineer to estimate the amount of water needed to suppress a fire in a given enclosure using conventional sprinklers. Since fine water spray or mist systems may have advantages over conventional sprinklers in specific applications, current research interest in the role of water in fire suppression has focused on such systems. One advantage of using water mist is the reduction in water demands, as much as an order of magnitude less than a conventional sprinkler system. As a result of less water flow, collateral damage by water will be less severe. Another advantage of fine water sprays is that several modes of fire suppression mechanism may be present when smaller water droplets are used. The predominant suppression actions of a conventional sprinkler are thought to be surface cooling and pre-wetting adjacent surfaces to inhibit flame spread, whereas the suppression mechanisms for fine water spray systems may include, in addition to surface cooling, flame cooling, thus causing reduction in flame radiation, diluting reactants with water vapor, and possible flame stretch through momentum transport between the spray and the fire plume.

The distinction between a water sprinkler and a water spray system is not well defined. In the spray literature (*e.g.*, Lefebvre, 1989), a system of drops having representative drop sizes greater than 1000 μm is classified as a "sprinkler." For systems with drop sizes ranged between 10 μm and 1000 μm , they are collectively referred to as "sprays" in which "mists" is a subset. A spray can further be classified as being "small (25 μm - 125 μm)," "median (50 μm - 250 μm)," or "coarse (150 μm - 600 μm)," according to Bayvel and Orzechowski (1993). In fire literature, "mist" most often is synonymous to "fine spray." As proposed by Mawhinney *et al.* (1994) and based on the volumetric mean diameter, D_{vx} (D_{vx} refers to x % of the total volume of the spray contained in drops below a given size), water sprays may be conveniently divided into three classes as follows:

Class 1 Spray: $D_{v10} < 100 \mu\text{m}$ and $D_{v90} < 200 \mu\text{m}$

Class 2 Spray: $D_{v10} < 200 \mu\text{m}$ and $D_{v90} < 400 \mu\text{m}$

Class 3 Spray: $D_{v10} > 200 \mu\text{m}$ and $D_{v90} > 400 \mu\text{m}$

Note that there is no scientific basis for the above spray classification.

Many full-scale fine water spray suppression tests have been conducted. For example, the effects of liquid fuel properties, preburn time (time between ignition and water application), spray properties, and direction of spray application on flame extinction have been carried out by Rasbash and co-workers (1957, 1960, 1962). The extinction time was found to decrease as the flow of water and the entrained air in the spray increased and generally as the drop size of the spray decreased from a mass median diameter (defined as the diameter below or above which lies 50 % of the total mass of the droplets) of 490 μm to 280 μm . If a stable flame was established following the spray application, it was very difficult to extinguish such flame when the preburn time (defined as the time between ignition and the initiation

of water application) was very short and when the spray was applied in a horizontal direction across the fire. Tamanini (1976a, 1976b) studied the extinguishment of vertical wood slab and wood crib fires using a water spray. Power law correlations were presented for the mass loss and the extinguishment time as functions of water application rate. The feasibility of applying fine water sprays to protect data processing equipment has been studied by Grosshandler *et al.* (1994). Fine water spray systems located external to simulated computer cabinets were found to be unlikely to be able to extinguish fires within the units anywhere near as effectively as a gaseous agent. The interaction of a low thrust water mist with a buoyant diffusion flame has been examined by Downie *et al.* (1994). It was observed that application of the spray resulted in a decrease in soot radiation, a decrease in oxygen concentration and an increase in CO concentration around the flame tip region. Within the experimental uncertainty, centerline flame temperatures did not change significantly upon application of the spray. Wighus and Aune (1995) presented some empirical engineering relations for water mist fire suppression systems. From experiments using open fires, they observed that when the spray heat absorption ratio, which was defined as the ratio of the heat absorbed by the vaporizing water mist to the heat produced by the fire, was greater than 0.3, the fire was likely to be extinguished by the water mist.

In spite of many full-scale tests, little has been done systematically to examine the effects of fuel configuration, fuel composition and properties, physical environment (*e.g.*, external radiative flux to the burning surface to simulate a real fire environment), and water droplet size and momentum on the performance of a fine water spray system. Magee and Reitz (1975) studied extinguishment of radiation augmented plastic fires using water sprays. The effect of external radiative heat flux on the extinguishment time was examined. However, the average droplet size used in most of the experiments was greater than 1 mm. The effect of droplet size on fine water mist suppression of a small liquid pool fire has been studied recently using micronozzle arrays by Alexander *et al.* (1994). Their results show that for a fixed water flow, the time to extinguishment is much shorter for a small nozzle than for a large one. For a fixed operating pressure, the large nozzle array extinguishes the fire faster than the small nozzle array. However, the droplet sizes and velocities could not be characterized in their experiments. Our work was an attempt to address the effects of some of the parameters in a well characterized, laboratory-type fire setting, and our focus was on solid combustibles, that included a thermoplastic (polymethyl methacrylate, PMMA), a foam (expanded polystyrene), and wood.

Specifically, the objective of this work was to examine how the orientation of a burning surface and its location relative to the spray nozzle affects the mass flux of droplets required to extinguish the flame. The effects of drop size and momentum were, to a lesser extent, also examined. The research effort was primarily focused on *low* pressure fine spray systems.

Since the criteria for classifying water mist systems are currently being developed by the National Fire Protection Association (NFPA) Water Mist Committee, the definition of a water mist has not yet been clearly established. For the purpose of this work, the proposed classification by Mawhinney *et al.* (1994) was used as a guide for designing the experiments. Two average droplet sizes were selected: one was in the neighborhood of 200 μm or less, and the other was above 400 μm but less than 1000 μm . The former size was dictated by the nozzle opening of the prototype spray generator (to be discussed), and the latter average size was chosen based on the measurements of droplet sizes from a commercial low pressure, high momentum pendant water mist nozzle which is currently being evaluated for protection of light hazard and residential areas.

There are two parts in this final report. The first, which is the main text, addresses various factors that may influence water requirements for extinguishing certain types of solid combustibles, and

the second, included in **Appendix C**, details the experimental results (drop size distribution measurements) obtained from the aforementioned commercial pendant nozzle.

2. Experimental Facility

Figure 1 shows a schematic of the experimental apparatus used to conduct the suppression tests. The facility consists of a conical heater, a sample holder, a load cell, and a water spray/droplet generating device. The facility is housed inside an enclosure (not shown in Figure 1) with a dimension of 2.0 m x 1.5 m x 0.9 m in order to prevent perturbation of the flame from forced ventilation in the laboratory. The enclosure is also equipped with proper ventilation to remove combustion products after each test.

2.1 Conical Heater

The heater was identical to those used in the NIST Cone Calorimeter and was capable of supplying a radiative heat flux of 25 kW/m² or more, depending on the transformer used and the distance between the heater and the sample. In typical Cone Calorimeter applications, the distance between the lower heater rim and the sample to be heated is about 5 cm. Unlike Cone operation, there was no fan-induced flow. In the suppression tests reported herein, a distance of 10 cm was used. This distance was chosen as a compromise between the required heat flux and prevention of splattering of water droplets onto the heater surfaces during water application.

2.2. Heat Flux Gauge

A Medtherm¹ heat flux gauge (Model No. GTW-3-32-485K) of the Schmidt-Boelter type was used to measure incident radiative heat flux to the sample surface from the cone heater. Water at room temperature was used to cool the gauge at a rate of 8.8 cm³/s during measurements. Output from the gauge was recorded using a voltmeter (Fluke 79) with an uncertainty of 0.1 mV (which corresponds to 0.4 kW/m²). The calibration curve provided by the manufacturer was used to convert voltage from the gauge to kW/m². Heat flux measurements were performed by placing the gauge at the same vertical distance between the sample surface and the lower rim of the cone heater and at locations corresponding to the center and the four corners of the sample surface. The measured heat fluxes at these five locations were found to deviate less than 5 %. Therefore, the incident radiative heat flux to the sample surface was considered uniform.

2.3 Sample Holder, Sample Materials, and Load Cell

The design of the sample holder was the same as that used in the NIST cone calorimeter except that the dimension was modified to accommodate a smaller sample. The sample materials used in the tests were polymethyl methacrylate (PMMA), solid white pine (No. 1), and a low density (32 kg/m³ non-fire retardant expanded) polystyrene foam. Sample size was 5 cm x 5 cm x 2 cm. For the polystyrene, two samples were placed on top of one another to obtain a longer burning time. Although a low density polyurethane had been tried in some of the preliminary tests, it was found that burnout time of the sample was too short to perform suppression tests even if a stack of three samples was used.

¹ Certain commercial products are identified in this report in order to adequately specify equipment used. Such identification does not imply recommendation from the National Institute of Standards and Technology, nor does it imply that this equipment is the best available for the purpose.

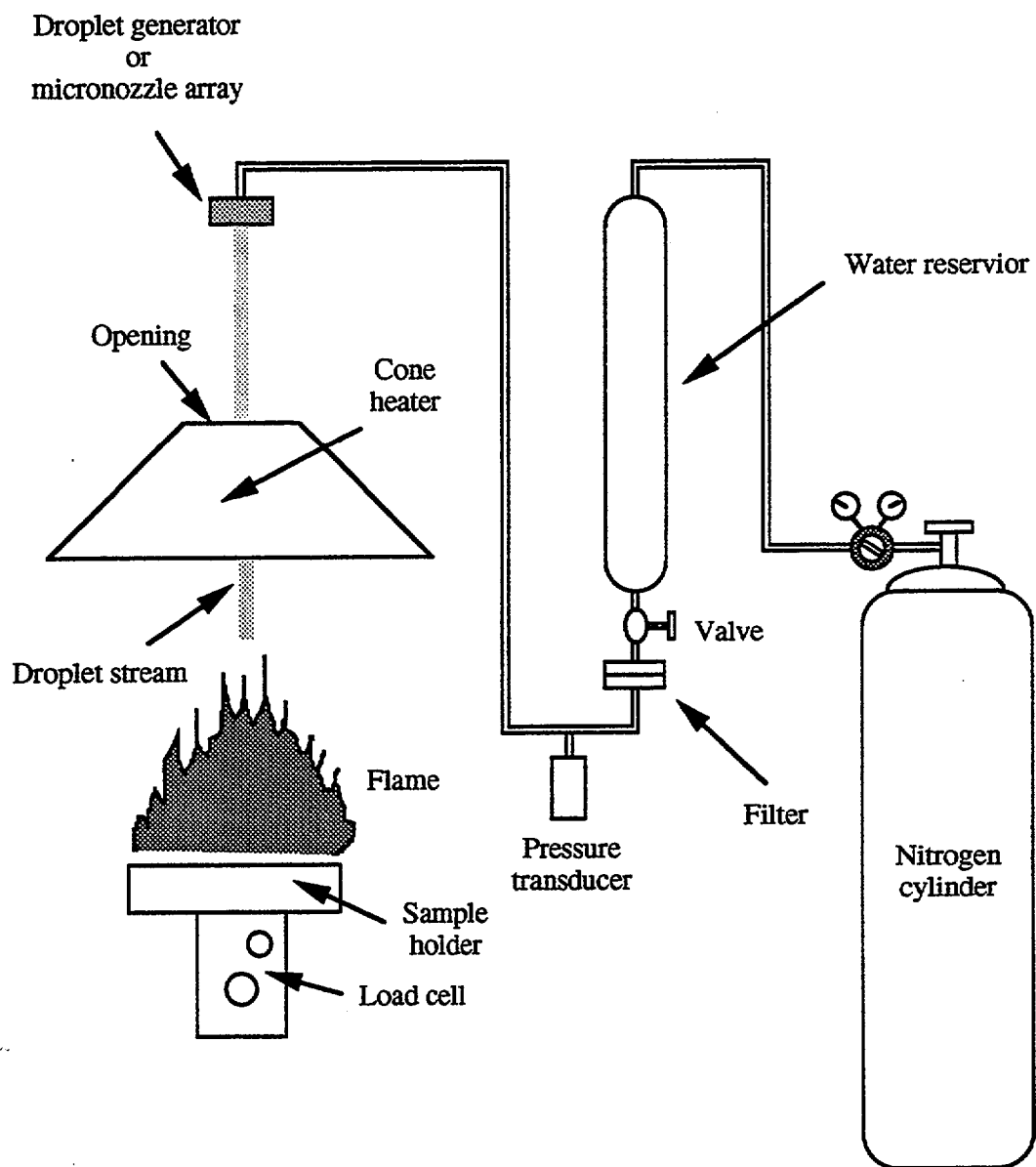


Figure 1. Schematic of the experimental set-up.

A load cell (Automatic Timing and Control, Inc. Model 6005D04E1xx) was used to monitor sample mass loss before water application. The voltage from the load cell was directed to a data acquisition system (Strawberry Tree, Flash-12) on a PC-486 computer, and average burning rates were obtained from the mass loss curves. Attempts to monitor mass loss during water application were not fruitful because of the large fluctuation of the load cell reading caused by the impact of the water stream on the burning sample surface and the comparable time scale between the response of the load cell and extinguishment time.

2.4 Droplet/Spray Generators

Two types of water droplet/spray generating devices were used in the experiments. To obtain small droplet sprays, an ITM micronozzle array was used. The array was a 1 cm x 1 cm x 0.075 cm silicon wafer with micronozzles (52 μm or 62 μm nominal opening) fabricated in the wafer. The current prototype provided by ITM, Inc. can accommodate 12 x 12 micronozzles on one wafer. Not all of the micronozzles were used in the experiments because the resulting water flow was too large for the suppression experiments. Only few micronozzles (fewer than five) were used in the experiments. The rest were blocked using fast-setting epoxy.

There are two modes of operation for these prototype arrays: (1) without nitrogen co-flow and (2) with nitrogen co-flow. Figure 2a shows a typical design of a micronozzle array without nitrogen co-flow. In this case, a pressurized water supply is connected to a manifold which channels water to the individual micronozzles. The droplet generation mechanism is based solely on instability breakup of water jets issuing from a small hole (Bayvel and Orzechowski, 1993) under the action of surface tension. When a liquid is forced through a nozzle with sufficient velocity, a liquid jet emanates from the nozzle and subsequently breaks into droplets downstream. The breakup distance is a function of jet velocity and fluid properties. Since the breakup process is not controlled by any external means, the resulting droplets vary in sizes and are not evenly spaced. In addition, close spacing of droplets will eventually cause adjacent drops to collide in the stream due to the differences in drag force caused by the trailing wakes of the falling droplets before they reach the sample surface. As a result of droplet collisions, coalescence and disintegration of parent droplets could occur, and the creation of a spray with a non-uniform drop size distribution results.

Figure 2b is a schematic of a micronozzle array with nitrogen co-flow. Two manifolds are used; one for water supply and one for nitrogen. The two manifolds are designed in such a way that each issuing water jet is surrounded by four issuing gaseous nitrogen jets. In this way, the nitrogen jets will facilitate the breakup of the water jet through shearing action, will reduce collision or coalescence of water droplets from adjacent water jets, and can be used to control or alter droplet size distribution with the *same* flow of water (to be discussed). The idea of using a gaseous flow to minimize droplet coalescence was first proposed by Dabora (1967) for production of monodisperse sprays.

For larger droplets, a piezoelectric droplet generator, a schematic of which is shown in Figure 3, was used. A piezoelectric bimorph diaphragm was mounted on one side of the chamber and was connected to a pulse generator (Hewlett Parkard Model 214B) which was able to control pulsing frequency and to supply pulse amplitude up to 100 V. The generator was operated at 100 V and 1 kHz. The nozzle was made by placing a Pyrex glass tube (2.9 mm o.d. and 1.4 mm i.d.) on the two rotating chucks of a small lathe. The middle portion of the tube was gradually shrunk by heating locally with a micro-torch while the two opposing chucks were turning and pulling away in opposition directions slowly without breaking the tube. The necked glass tube was then cooled and cut into two nozzles using a

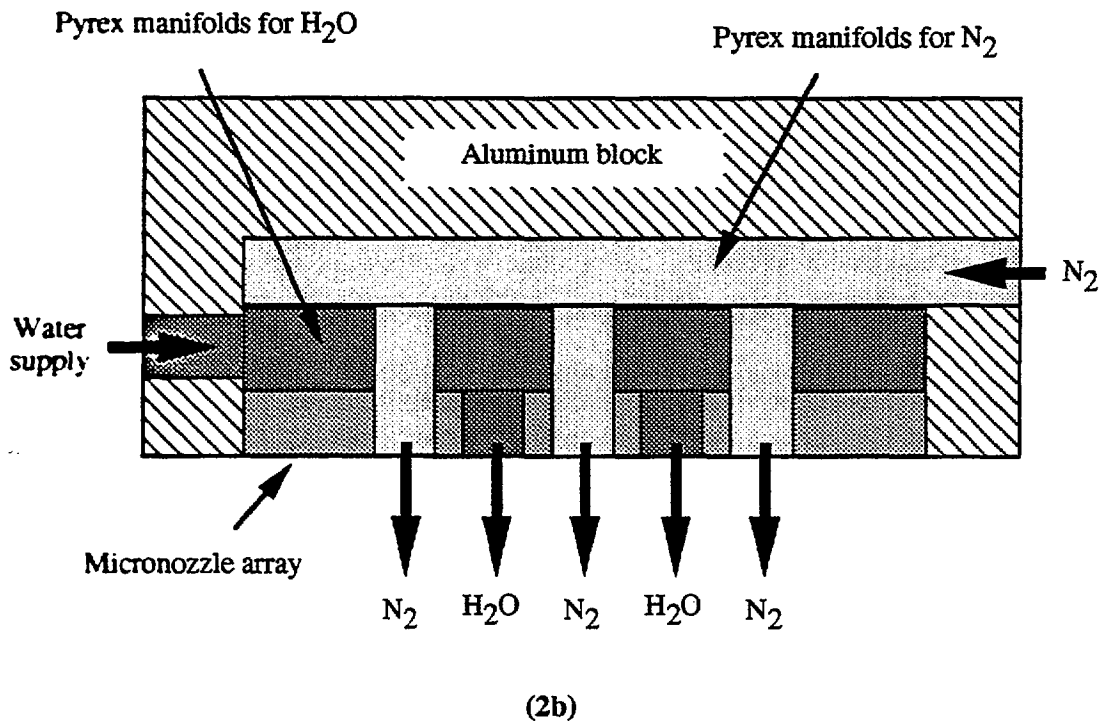
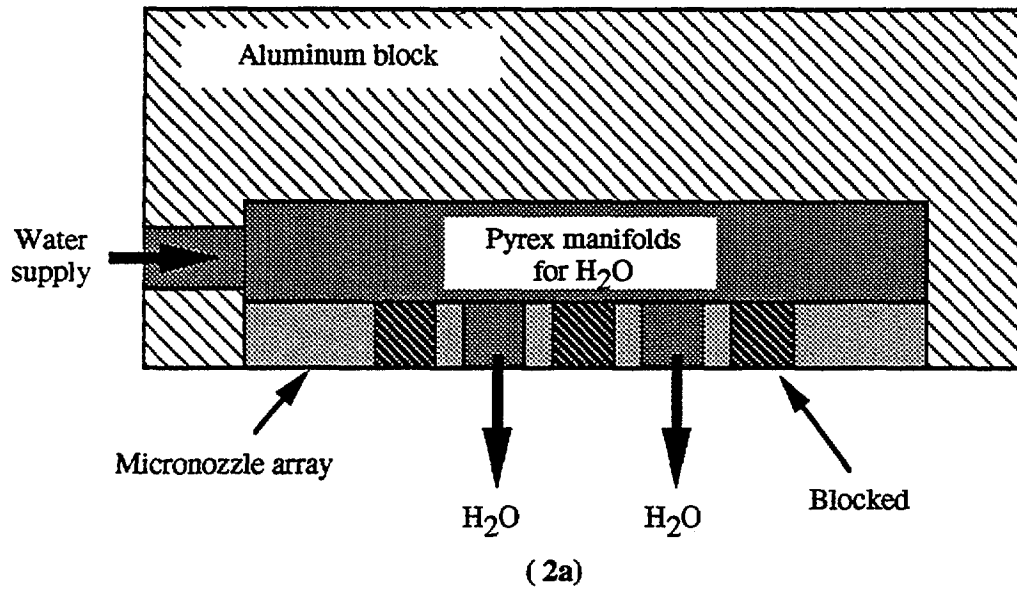


Figure 2. Schematic of micronozzle array.

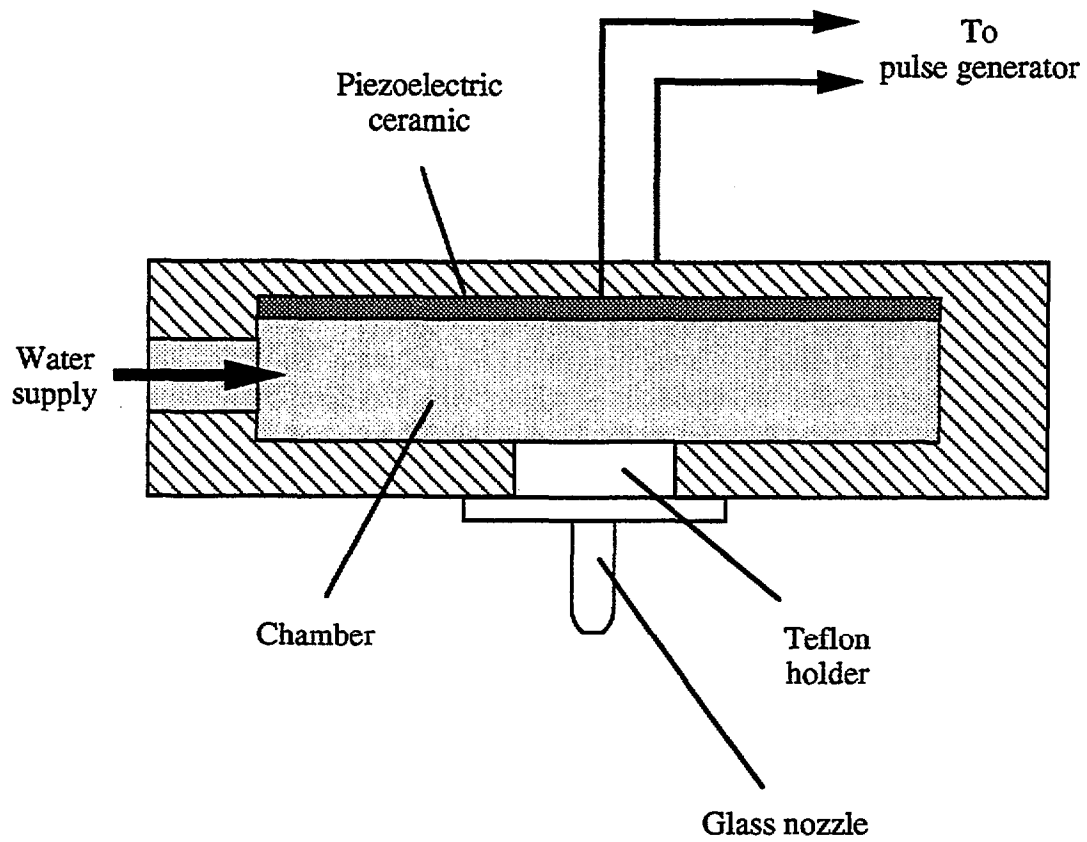


Figure 3. Schematic of the piezoelectric droplet generator.

carbide knife at the location of the neck. The two nozzle tips were then polished by using a glass sander. The nozzle opening used in the experiments reported herein was determined to be $280 \mu\text{m} \pm 40 \mu\text{m}$ as measured with a microscope with reticles.

The breakup of the water jet is facilitated and controlled by the vibrating piezoelectric ceramic. When a disturbance with controlled frequency and amplitude is applied to the emanating water jet, droplets with uniform size and even spacing can be obtained from subsequent jet breakup (Lindblad and Schneider, 1965; Berglund and Liu, 1973; Ashgriz and Yao, 1987). However, at a distance further downstream away from the breakup, spacings between droplets become random because of the differences in drag forces on individual droplets. As a result, droplets will eventually collide thus causing a non-uniform drop size distribution and a dispersed spray.

2.5 Water Flow System

Distilled, deionized water was used in all the experiments with a micronozzle array. Non-deionized water was used for the piezoelectric droplet generator. The reason for using high purity water was to prevent clogging of the small nozzle. A 500 ml stainless steel vessel was used as a water reservoir. To obtain a steady water flow, a constant head was maintained using nitrogen from a high-pressure cylinder. In all the experiments, the nitrogen pressure in the water reservoir was less than 0.21 MPa gauge. A 25 mm stainless steel line filter holder (Millipore XX45 025 00) with a $5 \mu\text{m}$ filter was also placed between the reservoir and the droplet/spray generator. A pressure transducer (Druck Model PDCR 330) with a resolution of 6.9 kPa was mounted between the filter outlet and the droplet generator. Volumetric water flow at a specified pressure was measured by collecting water at the droplet generator exit over a time interval using a container and a stop watch. The filled container was then weighed using an electronic scale with an uncertainty of 0.05 g to determine the mass of water collected and water flow rate.

2.6 Experimental Procedure

Most of the experiments conducted were recorded on video tapes for subsequent frame-by-frame analysis. The experimental procedure involved the following steps:

1. A receptacle was placed below the droplet/spray generator exit to prevent the droplet stream from impinging the sample surface. Water flow was then initiated by turning on the valve and was adjusted by regulating the nitrogen pressure in the water reservoir to obtain the desired flow rate for the experiments. Once the desired flow rate had been established, water flow was terminated by turning off the valve.
2. The sample holder with a sample was placed under the cone heater with a radiation shield between the holder assembly and the heater to prevent unwanted preheating of the sample during the transient startup of the cone heater.
3. When the cone heater reached its steady operation condition, the radiation shield was removed.
4. The sample was preheated under a constant heat flux from the cone heater for 60 s.
5. The preheated sample was then ignited using a pilot butane torch.

6. The sample was allowed to burn for 60 s before water application. A 30 s preburn time was used for polystyrene samples (refer to Section 3.3 for explanation).
7. During the preburn period, water flow was initiated (but shielded from sample) to ensure a steady flow before a suppression experiment was conducted.
8. At the end of preburn, the water retainer was removed in order to direct the droplet stream to the burning surface.
9. Extinction time was obtained by using a stop watch (for the micronozzle array experiments) or by counting frames from the video record obtained by using a CCD camera.

2.7 Experimental Conditions

The experimental parameters considered were type of sample material, water flow, external radiative heat flux, nozzle size, distance between nozzle and sample surface, and orientation of sample surface with respect to nozzle (see Figure 4). Table 1 summarizes the experimental conditions. The minimum water flow rates listed in the table were those that were necessary to form jets at the nozzles. Flow rates lower than the minimum frequently resulted in the formation of pendant drops at the nozzles. These drops subsequently detached and fell from the nozzle when their weight overcame surface tension.

3. Results and Discussion

3.1 Micronozzle Array Characterization

The ITM micronozzle arrays were characterized using a Phase Doppler Particle Analyzer (PDPA) from Aerometrics. The optical set-up and operating conditions of the PDPA were similar to those reported in Grosshandler *et al.* (1994). The characterization of the spray was performed in the absence of a fire. The size and velocity distributions at various selected locations were obtained. Table 2 summarizes the drop size and velocity measurements at 25 cm, 29 cm, and 55 cm from the 62 μm micronozzle array used in the experiments. It is clear that the droplet sizes obtained at the selected locations are not affected by different water pressures (flow rates) and the droplet axial velocity decreases slightly with distance at a given water flow rate.

Table 3 compares drop size distributions from the 52 μm micronozzle array operating with and without nitrogen co-flow. The droplet number densities at the measurement location were found to be 32.5 cm^{-3} (with co-flow) and 4.8 cm^{-3} (without co-flow). The co-flow significantly affects the mean droplet diameter and drop size distribution. This is an important finding because it provides a simple means for tailoring the average droplet size without changing any other operation parameters such as liquid flow rate, nozzle diameter, or number of nozzles.

3.2 Piezoelectric Droplet Generator Characterization

Since the current optical set-up in the PDPA was not designed for droplet sizes greater than 300 μm , the average droplet size from the piezoelectric droplet generator was characterized using stroboscopic photography. The set-up consisted of a Quadtech strobe (Model 1538A) and a Nikon F-4s 35 mm camera equipped with a 50 mm Nikkor lens and a close-up bellows (PB-6). Kodak Tmax 100 black and white

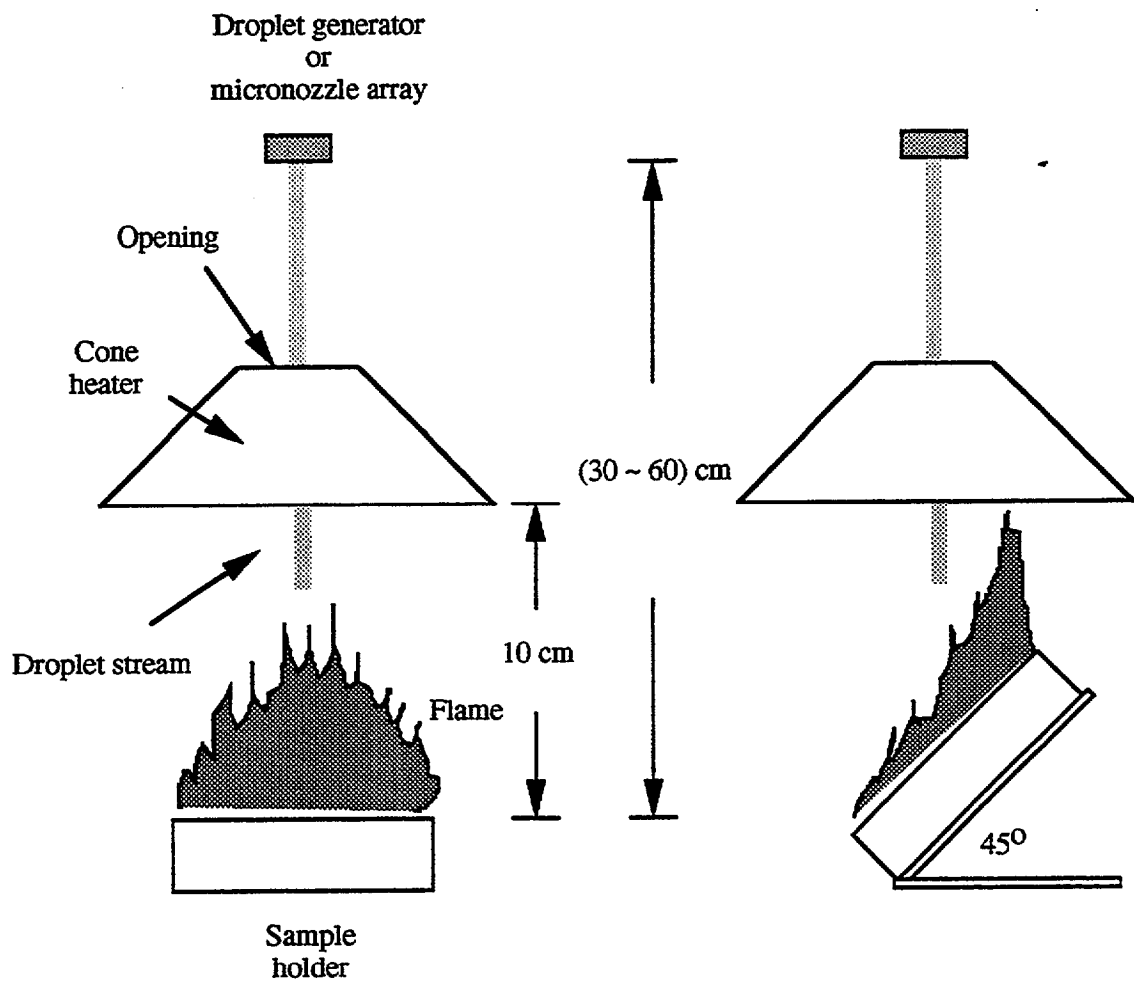


Figure 4. Sample-nozzle configuration.

Table 1. Experimental parameters

	Micronozzle array		Glass nozzle
Nozzle size (μm)	52	62	280
Number of nozzles	2	2	1
Water flow (cm^3/s)	0.06 - 0.20	0.07 - 0.18	0.42 - 1.80
Nozzle distance from sample surface (cm)	30 - 60	30 - 60	50 - 60
Nitrogen co-flow	Yes	No	N/A
Sample material	PMMA, Pine	PMMA, Pine	PMMA, Pine, PS foam
Nozzle orientation relative to sample surface	90°	90°	90° and 45°
External radiant flux (kW/m^2)	14	14	25

films were used. The droplet size at breakup was determined from the photographs. The droplet diameter at break-up was $600 \mu\text{m} \pm 150 \mu\text{m}$ for all conditions. The spread in the measurements resulted from the formation of satellite droplets and the dependence of droplet diameter on the jet velocity at a given excitation frequency (Ashgriz and Yao, 1987).

Since the droplet velocities were not measured, the terminal velocities of drops with diameters ranged from $200 \mu\text{m}$ to $1000 \mu\text{m}$ were calculated in order to provide estimates of droplet velocities. The terminal velocity, V_t , of a drop with a diameter D is obtained by equating the gravitational force to the sum of the buoyancy force and drag force acting on the drop:

$$\frac{4}{3} \pi R^3 \rho_l g = \frac{4}{3} \pi R^3 \rho_g g + \frac{1}{2} C_D \rho_g \pi R^2 V_t^2 \quad (1)$$

where R is the drop radius, g is the gravitational acceleration, ρ_l is the density of the drop, ρ_g is the density of the ambient gas, and C_D is the drag coefficient. An implicit assumption in Equation (1) is that the ambient gas through which the drop is travelling is stationary. Solving for V_t , the following equation for the drop terminal velocity is obtained:

Table 2. Drop size and velocity measurements from the 62 μm micronozzle array

Water flow rate (cm^3/s) $\pm 0.01 \text{ cm}^3/\text{s}$	Location of measurement from array (cm) $\pm 0.5 \text{ cm}$	Axial velocity (m/s) $\pm 0.5 \text{ m/s}$	Sauter mean diameter (μm) $\pm 20 \mu\text{m}$
0.09	25	7.1	214
0.14	25	12.0	213
0.18	25	13.9	213
0.09	29	-	219
0.14	29	10.0	212
0.14	29	-	217
0.18	29	13.4	212
0.14	55	4.6	200
0.18	55	6.8	205

$$V_t = \sqrt{\frac{4g(\rho_l - \rho_g)D}{3\rho_g C_D}} \quad (2)$$

The drag coefficient C_D is a function of the drop Reynolds number, Re ($\equiv V_t D \rho_g / \mu_g$ where μ_g is the viscosity of the ambient gas). In the range of $0 < Re \leq 2 \times 10^5$, C_D can be estimated by using the following equation (White, 1974):

$$C_D = \frac{24}{Re} + \frac{6}{1 + \sqrt{Re}} + 0.4 \quad (3)$$

Equations (2) and (3) can be solved using a Newton-Raphson iterative scheme (Press *et al.*, 1992) to obtain the terminal velocity. For water drops with diameters of 200 μm , 400 μm , 600 μm , 800 μm , and 1000 μm , the corresponding terminal velocities in stationary air at 298 K are calculated to be 0.66 m/s, 1.50 m/s, 2.20 m/s, 2.87 m/s, and 3.44 m/s respectively.

3.3 Mass Burning Rates

Burning rates of PMMA and white pine samples under different external radiant heat fluxes were measured and are listed in Table 4. Because of the low density of this polystyrene foam, it became very

Table 3. Drop size and velocity measurements at 55 cm from the 52 μm micronozzle array

Water flow rate (cm^3/s)	Co-flow N_2 pressure (MPa)	Axial velocity (m/s)	Sauter mean diameter (μm)	Number density (cm^{-3})
0.17	0	3.7	201	4.8
0.17	0.275	3.1	164	32.5

difficult to obtain average burning rates by monitoring the temporal mass loss using a load cell in such a short duration before complete consumption of the sample or self-extinction (due to heat loss to the sample holder and char formation) occurred. For the polystyrene foam, the mass before ignition was first obtained by weighing. After preheating for 30 s, the sample was ignited and burnt for 60 s before the flame was extinguished by placing a marinite board on top of the burning sample. The time from ignition to flame suppression was recorded using a digital stop watch with an accuracy of 0.01 s. The residual sample was weighed using an electronic balance with an uncertainty of 0.01 g to obtain total mass loss of the foam. The average mass burning rate was defined as the ratio of sample mass loss to the total burning time. Note that there is an inherent assumption that sample mass loss was negligible during the preheating period. This technique was also used to obtain the average mass burning rates of PMMA and white pine. The differences in burning rates obtained from this technique and from the temporal mass loss curves were found to be less than 5 %.

3.4 Extinguishment Tests

The results obtained from the extinguishment tests were expressed in terms of extinguishment times. The extinguishment time is defined here as the time from the initiation of water application to the disappearance of a *visible* flame above the sample surface. In the early phase of the project, extinguishment times were measured using a stop watch with a resolution of 1/100 s and the eyes of the operator. The uncertainties associated with the measurements were estimated to be at least 0.2 s. All the tests using the micronozzle arrays were conducted in this manner. For experiments using the piezoelectric droplet generator, a CCD camera (Panasonic WV-CD 110A) was used to record the extinguishment events onto VHS tapes for subsequent frame-by-frame analysis. The uncertainties were estimated to be 0.1 s.

3.4.1 Phenomenological Description of Flame Extinguishment Process

For PMMA and white pine samples, visual observations revealed the following processes. At the instant when the droplet stream first impacted the sample surface, local flame extinction was immediately observed at the point of impact, the flame was perturbed by the arrival of the droplet stream, and flame luminosity was reduced. As the droplet stream continued impinging the sample surface, a water layer began to form, spread across, and wet the horizontal sample surface, and the ejection of droplets from the water layer occurred as a result of splattering of the droplet stream on the layer. The trajectories and directions of splash droplets and the resulting "wetness" of the surrounding area depend on the depth of the layer from which the droplets originate (Allen, 1988). The spreading of the water

Table 4. Average mass burning rates

External radiant heat flux (kW/m ²)	Average mass burning rate (g/s)			Sample orientation
	PMMA	White pine	Polystyrene foam	
14	0.023	0.015	N.A.	Horizontal
25	0.028	0.018	0.012	Horizontal
25*	0.017	0.013	N.A.	45° inclined

*Measured at the center of the sample

layer was not uniform because the sample surface was not perfectly smooth due to char formation (for white pine) or bubbling (for PMMA) and the surface temperature might not be uniform. Flame size was gradually reduced, and eventually total extinguishment resulted. For an inclined sample (45° with respect to the impinging droplet stream), several abnormalities were noted. Depending on the directions and trajectories of the splash droplets resulting from droplet stream impingement upon the water layer flowing along the inclined sample surface, total flame extinguishment *sometime* was not possible, with water application lasting for more than 3 min. If a significant portion of the splashed droplets landed on the down-slope side of the impinging stream, then small ghost flames were frequently observed to persist at the top of the inclined sample.

For the polystyrene foams, the sample first receded from all sides, curved inward from the edges and subsequently formed a viscous blob during preheating and upon ignition. Since the sample changed its shape in a random and unpredictable manner before the application of water, the droplet stream *sometime* did not directly impinge on the burning blob but instead impacted on the sample holder which resulted in a puddle of water. Total extinguishment of the flame was due to droplets splattering on the burning blob as the stream impacted on the pool of water and the spreading of the water puddle which eventually cooled the base of the burning foam.

Although flame extinguishment mechanisms by water mist have been suggested to be (1) heat extraction (flame cooling and fuel surface cooling), (2) oxygen displacement (or dilution), and (3) radiation attenuation (Mawhinney *et al.*, 1994), it is difficult to differentiate the relative importance of these three mechanisms.

If one assumes that direct flame cooling is due primarily to the extraction of heat from the flame to vaporize the fuel (to simplify the discussion, superheating of the steam generated is not considered), the residence times of water droplets in the flame zone (or their times of flight through the flame zone) would determine whether flame cooling is the dominant mechanism to suppress the flame. If the residence time of a droplet is longer than its evaporation time in the flame zone, then the droplet will vaporize completely before it reaches the fuel surface. In this case, flame cooling could be significant. On the other hand, if the residence time is shorter than the complete vaporization time, the droplet mass may not be reduced significantly through vaporization. Under this circumstance, significant flame cooling may not be realized.

Direct flame cooling is thought not to be very significant in most of our tests because the residence times of individual droplets in the flame zone were much shorter than the characteristic times for droplet heating and complete evaporation. Since the temperature of the droplet when introduced into the flame zone has not yet reached its final, equilibrium value, there is an initial transient droplet heating period. For a small droplet, say 200 μm in diameter (see Tables 2 and 3), exposed to an ambience of 1700 K and assuming a lump capacitance model (Incropera and DeWitt, 1985), the characteristic droplet heat-up time is estimated to be of the order of 0.1 s. The flame height was of the order of 10 cm based on visual observations. The droplet velocity typically was of the order of 10 m/s or less in our experiments (see Tables 2 and 3). Therefore, the residence time of the droplet in the flame zone typically was of the order of 0.01 s. For a 200 μm droplet evaporating at an ambience of 1700 K, the complete evaporation time of the droplet was estimated by using the classical d^2 -law (see *e.g.*, Spalding, 1979) to be at least an order of magnitude (~ 0.1 s) more than the residence time. Therefore, droplet mass loss due to evaporation by extraction of heat from the flame could be considered negligible in the flame zone, and significant flame cooling was unlikely. However, the water vapor generated at the sample surface and superheating of the vapor could cool the flame near the surface. In the experiments using the micronozzle array with nitrogen co-flow, flame cooling could play a slightly larger role in the flame extinguishment process because the surface area available for evaporation increased as a result of an increase in droplet number density and the droplet sizes were smaller.

Radiation blockage by droplets does not play a role in extinguishing our flames because at most two droplet streams were used in the experiments and the space occupied by the streams was only a small fraction of the total flame volume. Oxygen displacement due to the generation of water vapor *within* the flame zone as a result of droplet vaporization would also not contribute significantly to the flame extinction process, based on the residence times argument.

Therefore, it is postulated that the observed flame extinction in the experiments was due largely to fuel surface cooling. As the droplet stream continued impinging the sample surface, cooling of the surface occurred because of the heat transfer between the sample surface and water droplets deposited on the surface. As the surface temperature decreased, the evaporation rate of water droplets and the gasification rate of the sample decreased. A water layer began to form due to continuous droplet deposition on the surface and reduced evaporation rate. The layer, which spread and grew, further reduced the exposed sample surface and the surface temperature by wetting. Eventually, a condition was reached that the sample gasification rate was so low that combustion could not be sustained, and total flame extinguishment resulted.

3.4.2 Micronozzle Array Results

Figure 5 shows the extinguishment time as a function of water flow for the 62 μm micronozzle array. The water droplet stream was applied perpendicular to the sample surface. Nitrogen co-flow was not used in these experiments. An external radiant heat flux of 14 kW/m^2 was used. Two sets of data are shown in the figure. One set was taken with the array located 30 cm above the sample surface and the other set with the array at 60 cm. White pine and PMMA were used in these tests. Each data point in Figure 5 is the average of at least three runs, and the error bars in the figure represent the standard deviations. A complete set of the experimental data can be found in **Appendix A**.

In Figure 5, the extinguishment time decreases with increasing water volumetric flow. The extinguishment time is much longer for PMMA fires than for white pine fires because the gasification rate of white pine decreases due to char formation during the 60 s preburn before water application.

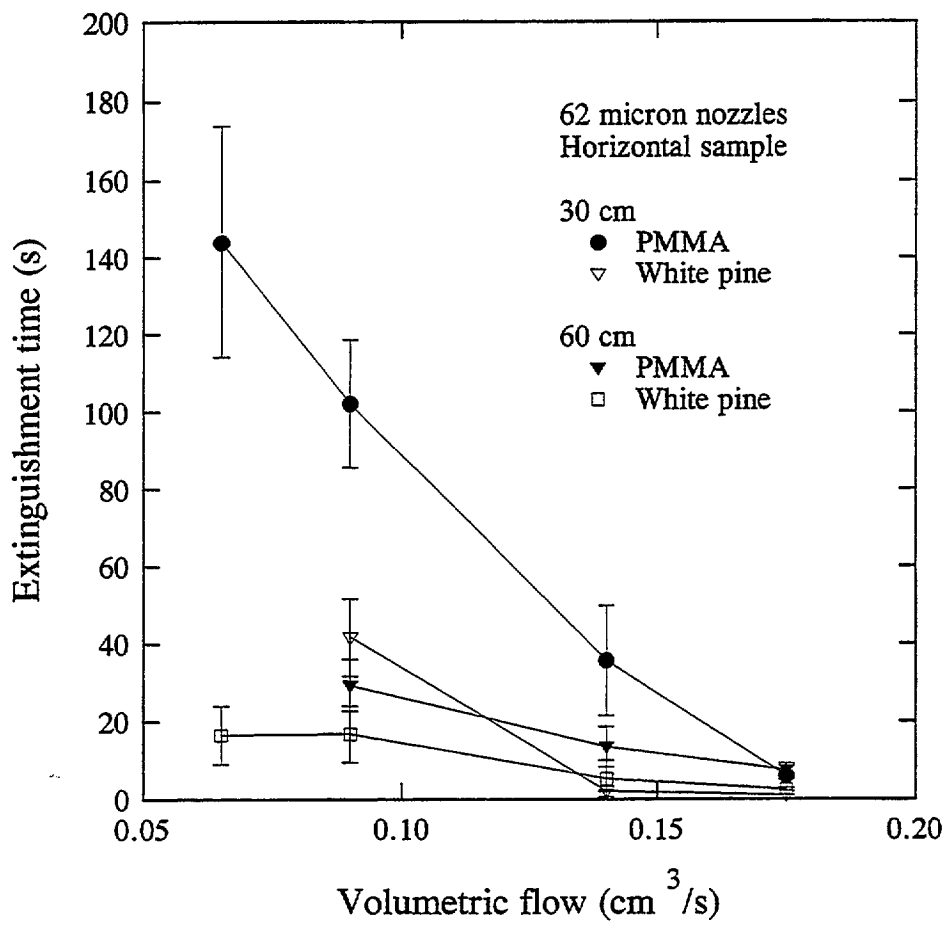


Figure 5. Average extinguishment time versus volumetric water flow for white pine and PMMA. The 62 μm micronozzle array was located at 30 cm or 60 cm above the fuel surface.

When the array is located further from the sample surface (60 cm), the extinguishment times are, on average, shorter at *very low* water flow than those obtained when the array is located closer to the sample surface (30 cm). One plausible explanation is as follows. When the array is further from sample surface, droplets in the stream have sufficient time to interact with one another before their arrival to the sample surface. The droplet interaction processes appear to enhance the dispersion of droplets and the coverage area of the droplet stream even though the initial droplet velocities are slow due to low exit water flow rate from the micronozzles. The greater water application coverage area facilitates flame extinguishment.

Figure 6 summarizes the extinguishment tests for the 52 μm micronozzle array using PMMA and an external radiant flux of 14 kW/m^2 . The data clearly show a very dramatic decrease in the extinguishment times when nitrogen co-flow is present, independent of the water flow rate and distance between the array and sample surface. However, due to the unusual large scatter of the data, the effect of water flow on the extinguishment time is not as apparent as that shown in Figure 5. The decrease in the extinguishment time could not be due to the flow of nitrogen *per se* because at a location of 40 cm above the sample surface, experiments were conducted with the flow of nitrogen (without co-flowing with water) from the array, and it was found that the presence of nitrogen did not even perturb the flame. Therefore, the only action of nitrogen co-flow was to facilitate the dispersion of droplets, to increase droplet impingement area, and to reduce droplet sizes given the same water flow. Since the coverage area of the droplet stream was affected slightly by the nitrogen co-flow, the decrease in extinguishment time can be attributed to the combined effect of enlarged spray coverage area and decreased average droplet diameter.

Close examination of the PMMA data presented in Figures 5 and 6 (at 60 cm nozzle location and without co-flow) shows some inconsistency in the effect of droplet size on extinguishment time. According to the above discussion, the 52 μm nozzle array should extinguish the flame more quickly than the 62 μm nozzle array. However, it can be argued that the effect of droplet size cannot be clearly demonstrated due to the small difference in nozzle opening and the large scatter of the data.

3.4.3 Piezoelectric Droplet Generator Results

The test results using the piezoelectric droplet generator are summarized in Figures 7, 8, and 9 for the two sample orientations and nozzle distances from the sample surface. The data shown in these figures are average values of at least three runs. A complete set of the experimental results is included in **Appendix B**.

For a horizontal sample, despite some scatter in the data, the extinguishment time in general decreases with increasing water flow, irrespective of the distance between the nozzle and the sample surface and sample orientation. The average extinguishment times for white pine samples are much shorter than those for PMMA and PS foam samples at low water flow rates. At low water flows, the extinguishment time decreases with increasing nozzle-to-surface distance when the sample is in a horizontal position with respect to the droplet stream. However, the effect of nozzle location is not apparent when the sample is placed in an inclined position (45°) relative to the droplet stream.

From the data, it is inferred that the extinguishment time will eventually reach an asymptote as the water flow rate increases, implying that there is a critical water flow rate for minimum extinguishment time. Further increase in water flow beyond this critical value may not reduce the extinguishment time significantly.

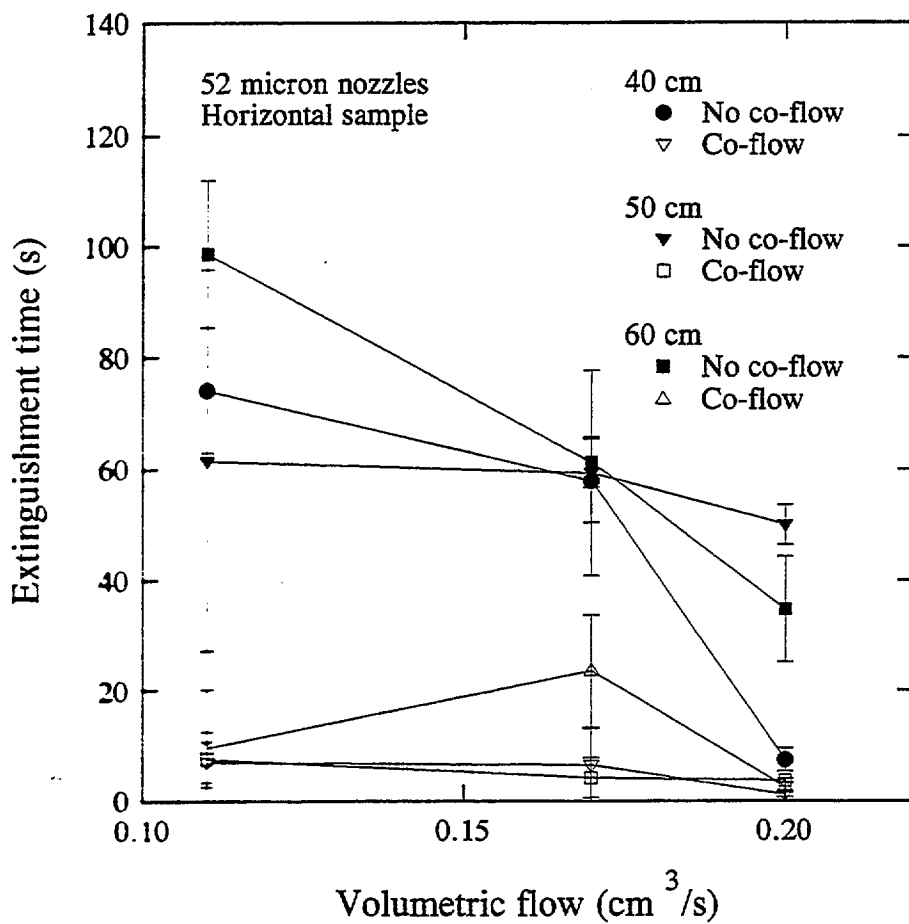


Figure 6. Average extinguishment time as a function of volumetric water flow for PMMA with and without nitrogen co-flow. The 52 μm micronozzle array was located at 40 cm, 50 cm, or 60 cm above the fuel surface.

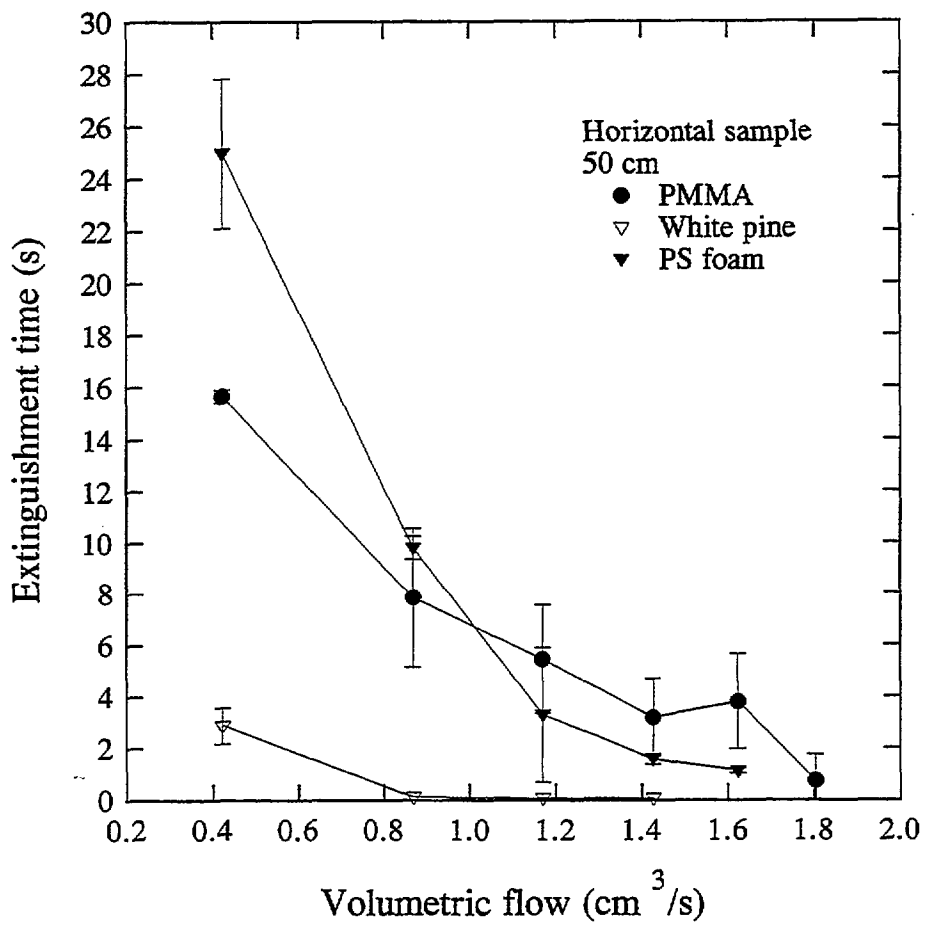


Figure 7. Average extinguishment time as a function of volumetric water flow. The glass nozzle was located at 50 cm above the sample surface.

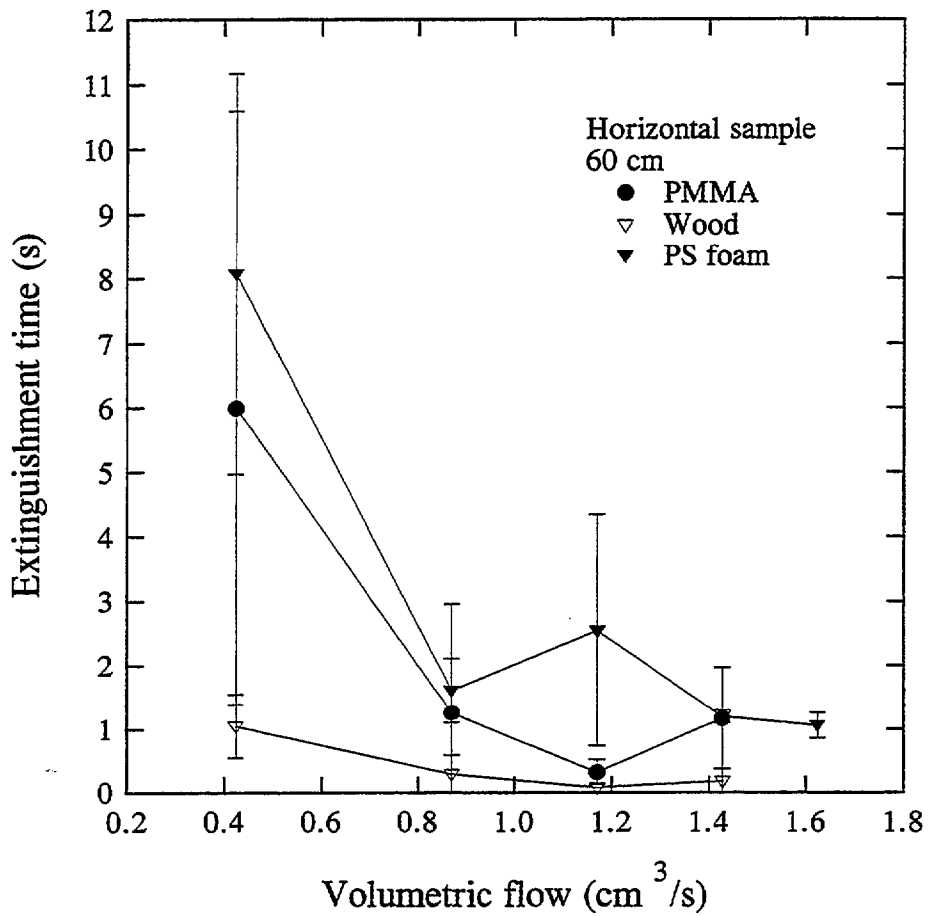


Figure 8. Average extinguishment time as a function of volumetric water flow. The glass nozzle was located at 60 cm above the sample surface.

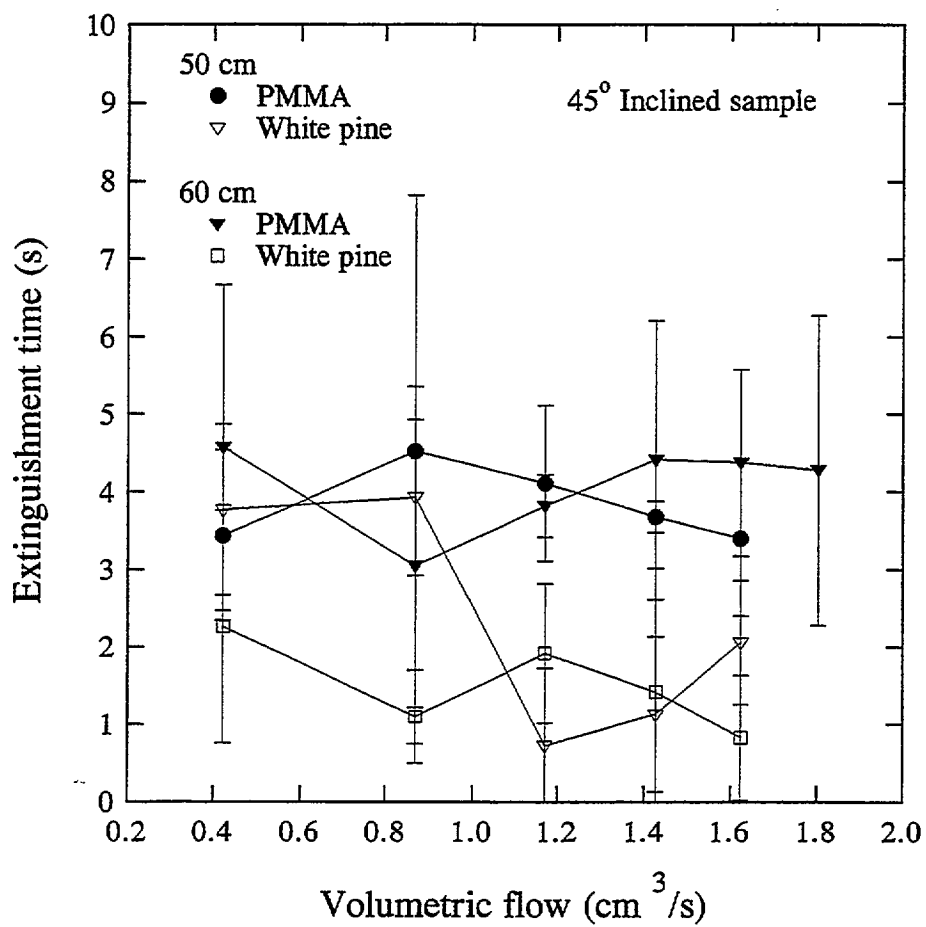


Figure 9. Average extinguishment time as a function of volumetric water flow. The glass nozzle was located at 50 cm or 60 cm above the sample surface. The sample was inclined at 45° with respect to the droplet stream.

3.4.4 Surface Cooling by Water

Based on the experimental observations, a simplified physical model is used to discuss suppression using water droplets/sprays on condensed-phase fuels. The objective here is to attempt to delineate some of the important physical mechanisms involved and to provide some heuristic explanations of the effects of the experimental parameters on extinguishment *via* surface cooling.

Rather than resorting to a detailed analysis (which proves to be very difficult) of flame extinction coupled with the transient thermal response of the fuel bed due to water application, a steady-state energy balance at the fuel surface is used to elucidate some of the underlying mechanisms.

In the absence of water application, a steady-state energy balance at the fuel surface can be written as

$$m_{fo}'' L_f = Q_e'' + Q_{conv}'' + \varepsilon_f \sigma T_f^A - \varepsilon_s \sigma T_s^A \quad (4)$$

where m_{fo}'' is the gasification mass flux prior to water application, L_f is the effective heat of gasification, Q_e'' is the imposed external heat flux, Q_{conv}'' is the convective heat flux, ε_f is the flame emissivity, σ is the Stefan-Boltzmann constant, T_f is the average flame temperature, ε_s is the surface emissivity, and T_s is the surface temperature.

When a water spray is present, two things can happen. If insufficient water is applied to the surface and if the water accumulation rate on the surface is balanced by its evaporation rate from the surface, then extinguishment cannot be realized. Continuous water application will ultimately lead to a new steady-state burning (Magee and Reitz, 1975). On the other hand, when sufficient water is applied to the surface and given enough time, the fire will eventually be extinguished.

If the action of water is treated simply as surface cooling and if water application is insufficient to extinguish the flame, then the surface energy balance at a new steady state is

$$m_f'' L_f = Q_e'' + Q_{conv}'' + \varepsilon_f \sigma T_f^A - \varepsilon_s \sigma T_s^A - \eta m_w'' [L_w + C_{pw} (T_{sat} - T_o)] \quad (5)$$

where m_f'' is the gasification mass flux, L_w is the heat of vaporization of water at T_{sat} (the saturation temperature of water), T_o is the initial water temperature, m_w'' is the water application flux, C_{pw} is the specific heat of liquid water, and η is the cooling efficiency of the water spray, a term used in spray cooling literature (*e.g.*, Bolle and Moureau, 1981). If all the water deposited on a unit surface area were vaporized instantaneously, then η is equal to 1. The cooling efficiency, η , is defined as

$$\eta = \frac{Q_w''}{m_w'' [L_w + C_{pw} (T_{sat} - T_o)]} \quad (6)$$

where Q_w'' is the actual heat removal or cooling rate per unit area due to the presence of water. The cooling efficiency is a function of impinging water drop size, surface superheat ($T_s - T_{sat}$) where T_s is the surface temperature, and other parameters. For water impinging on a heated stainless steel surface and if the viscosity of water is not considered, the cooling efficiency can be expressed as a function of three dimensionless parameters only in the transition and non-wetting or film boiling regimes (Liu and Yao, 1982).

$$\eta = \eta(We, B, K_d) \quad (7)$$

$$We = \frac{\rho_l D U^2}{\sigma_l} \quad (8)$$

$$B = \frac{C_{pv}(T_s - T_{sat})}{L_w} \quad (9)$$

$$K_d = \frac{k_v}{C_{pv} \rho_l \nu_l} \quad (10)$$

where We is the drop Weber number, subscript l represents liquid phase, D is the drop diameter, U is the drop impact velocity, σ_l is the surface tension, C_{pv} is the specific heat of water vapor, k_v is the thermal conductivity of water vapor, and ν is the kinematic viscosity.

Many suppression criteria have been used in the literature. For example, Williams (1974) discussed fire suppression from the viewpoint of a critical Damköhler number (defined as the ratio of the residence time of the reactants in the flame to the chemical reaction time) below which extinction occurs abruptly. Corlett and Williams (1975) introduced a length scale of coherent flaming with successful suppression being considered as reduction of the coherent length below a critical value. Rasbash (1962, 1986) discussed extinguishment using water in terms of fire point (which is defined as the temperature below which diffusional burning can no longer be possible). Recently, Delichatsios (1995) used critical pyrolysis rates to analyze extinguishment processes of solid fuel fires using water. Critical pyrolysis rate, $m_{f,cr}''$, is defined as the minimum pyrolysis rate for which steady burning exists. If m_f'' from Equation (5) is less than $m_{f,cr}''$, then extinguishment occurs abruptly.

When extinguishment is dominated by fuel surface cooling, the effects of water drop size and nozzle distance on extinguishment time may be explained in terms of the cooling efficiency, η , because η depends on drop size distribution and drop impact velocity, which is a function of the distance between the nozzle and the sample surface. Since cooling efficiency also depends on other parameters (*e.g.*, angle of drop impingement, splashing, surface roughness), it is conceivable that η may offer some plausible

explanations for the experimental results from the incline samples. Unfortunately, empirical correlations for obtaining η under conditions encountered in fires are lacking.

4. Conclusions

The average droplet sizes used in the experiments were chosen based on the drop size measurements from a commercial low pressure, high momentum pendant nozzle (refer to **Appendix C**). With these sizes, the smallest attainable volumetric flows from the droplet/spray generators always result in extinguishment of the flame. Thus, it was not possible to determine the minimum water flux for extinguishment from these sets of experiments. However, based on the experimental observations using micronozzle arrays and a single glass nozzle, some important conclusions can still be drawn.

- The time required for extinguishment generally decreases with increasing water application rate, irrespective of the nozzle distance from the burning surface. The extinguishment time appears to approach an asymptotic value as the water flow rate increases.
- For a given water flow, the time required for extinguishment decreases when a spray with smaller droplet size is used.
- At low water flows, the extinguishment time, in most cases, decreases when the nozzle is positioned further from the *horizontal* sample surface. On the contrary, at high water flow, the extinguishment time appears to be independent of the distance between the nozzle and the sample surface.
- For inclined samples, the extinguishment time does not seem to change significantly at the two nozzle-to-surface distances.
- Flame extinguishment is due primarily to fuel surface cooling and wetting in these sets of experiments.
- The above arguments and observations suggest that water mist systems that produce the majority of the droplets whose residence times in the fire zone are *shorter* than the evaporation times may perform similarly to a conventional sprinkler; that is, flame suppression action is due mainly to fuel surface wetting.

It should be noted that most of the (high pressure) water mist systems produce droplets with sizes much smaller than those used in this work (a low pressure configuration) and that in a realistic fire scenario the nozzle-sample distance is likely to be much greater than those used in the present study. Under these circumstances, the main suppression mechanism is likely to be flame cooling as a result of smaller droplet sizes and longer droplet residence times in the fire zone. Despite the difficulties associated with the direct interpretation of flame extinguishment processes of a real fire in terms of the results obtained from a laboratory scale fire, the work presented here proves to be valuable in deducing various controlling parameters (*e.g.*, drop size and sample orientation with respect to the nozzle) which may influence the suppression action of a water mist system in a real scale fire.

5. Recommendations

This study has identified the importance of drop diameter and nozzle location on flame extinction in small-scale laboratory fires. Further studies on the effects of these parameters are warranted in real scale fires. Since a water spray has a wide spectrum of drop sizes and velocities and if fuel surface cooling is the dominant suppression mechanism, detailed spray characterization near the fuel surface is required in order to understand the interaction of water drops with the surface. For given fuels, nozzle locations, and external heat fluxes, experiments with controlled drop size and velocity distributions need to be performed to determine the optimal distributions for extinguishment and to provide useful engineering data for subsequent development of engineering correlations which will enable prediction of suppression performance of a given water spray system.

6. References

- Alexander, T., NIST, Personal Communication (1994).
- Allen, R.F., "The Mechanics of Splashing," *J. Colloid & Interface Sci.* 124, 309 (1988).
- Ashgriz, N. and Yao, S.C., "Development of a Controlled Spray Generator," *Rev. Sci. Instrum.* 58(7), 1291 (1987).
- Bayvel, L. and Orzechowski, Z., "Liquid Atomization," Taylor and Francis, Washington DC, 1993.
- Berglund, R.N. and Liu, B.Y.H., "Generation of Monodisperse Aerosol Standards," *Environ. Sci. Tech.* 7, 107 (1973).
- Bolle, L. and Moureau, J.C., "Spray Cooling of Hot Surfaces," in *Multiphase Science and Technology*, Volume 1, Hewitt, G.F., Delhaye, J.M., and Zuber, N. (eds.), pp. 1-93, Hemisphere Publishing Co., Washington, DC, 1981.
- Corlett, R.C. and Williams, F.A., "Modeling Direct Suppression of Open Fires," *Fall Meeting of the Western States Section of the Combustion Institute*, Menlo Park, California, October 20-21, 1975.
- Dabora, E.K., "Production of Monodisperse Sprays," *Rev. Sci. Instrum.* 38(4), 502 (1967).
- Delichatsios, M.A., FMRC, Personal Communication (1995).
- Downie, B., Polymeropoulos, C.E., and Gogos, G., "Interaction of a Low Thrust Water Mist with a Buoyant Diffusion Flame," *Annual Conference on Fire Research*, October 17-20, 1994.
- Grosshandler, W.L., Lowe, D., Notarianni, K., and Rinkinen, W., "Protection of Data Processing Equipment with Fine Water Sprays," NISTIR 5514, October 1994, U.S. Department of Commerce, Washington, DC.
- Incropera, F.P. and DeWitt, D.P., *Fundamentals of Heat and Mass Transfer*, 2nd edition, John Wiley & Sons, New York, 1985.

- Lefebvre, A.H., *Atomization and Sprays*, Taylor & Francis, Pennsylvania, 1989.
- Lindblad, N.R. and Schneider, J.M., "Production of Uniform-Sized Liquid Droplets," *J. Sci. Instrum.* 42, 635 (1965).
- Liu, L. and Yao, S.C., "Heat Transfer Analysis of Droplet Flow Impinging on a Hot Surface," in *Heat Transfer 1982, Proceedings of the Seventh International Heat Transfer Conference*, Volume 4, Grill, U., Hahne, E., Stephan, K., and Straub, J. (eds.), Hemisphere Publishing Co., Washington, DC, 1982.
- Magee, R.S. and Reitz, R.D., "Extinguishment of Radiation Augmented Fires by Water Sprays," *15th Symp. (Int.) on Combustion*, pp. 337-347, the Combustion Institute, PA, 1975.
- Mawhinney, J.R., Dlugogorski, B.Z., and Kim, A.K., "A Closer Look at the Fire Extinguishing Properties of Water Mist," *Proceedings of the Fourth International Symposium in Fire Safety Science*, pp. 47-60 (1994).
- Press, W.H., Teukolsky, S.A., Vetterling, W.T., and Flannery, B.P., *Numerical Recipes*, 2nd edition, Cambridge University Press, Cambridge, 1992.
- Rasbash D.J. and Rogowski, Z.W., "Extinction of Fires in Liquids by Cooling with Water Sprays," *Comb. Flame* 1, 453 (1957).
- Rasbash D.J., Rogowski, Z.W., and Stark, G.W.V., "Mechanisms of Extinction of Liquid Fires with Water Sprays," *Comb. Flame* 4, 223 (1960).
- Rasbash, D.J., "The Extinction of Fires by Water Sprays," *Fire Res. Abstr. Rev.* 4(1), 28 (1962).
- Rasbash, D.J., "The Extinction of Fire with Plain Water: A Review," *Proceedings of the First International Symposium in Fire Safety Science*, pp. 1145-1163 (1986).
- Spalding, D.B., *Combustion and Mass Transfer*, Pergamon Press, Oxford, 1979.
- Tamanini, F., "A Study of the Extinguishment of Vertical Wood Slabs in Self-sustained Burning by Water Spray Application," *Comb. Sci. Technol.* 14, 1 (1976a).
- Tamanini, F., "The Application of Water Sprays to the Extinguishment of Crib Fires," *Comb. Sci. Technol.* 14, 17 (1976b).
- White, F.M., *Viscous Fluid Flow*, McGraw-Hill, New York, 1974.
- Wighus, R. and Aune, P., "Engineering Relations for Water Mist Fire Suppression Systems," *Halon Options Technical Working Conference Proceedings*, pp. 397-409, Albuquerque, New Mexico, May 9-11, 1995.
- Williams, F.A., "A Unified View of Fire Suppression," *J. Fire and Flammability* 5, 54 (1974).

Appendix A

Tables A-1 and A-2 list all the experimental data obtained by using micronozzle arrays. The data were taken with sample surface perpendicular to downward droplet streams and an external radiative heat flux of 14 kW/m². PS foam samples were not used in these tests.

Table A-1. Experimental data set for 62 μm micronozzle array

Sample	Nozzle distance (cm)	Water flow (cm ³ /s)	t_{ex} (s)	\pm SD (s)	$t_{ex, min}$ (s)	$t_{ex, max}$ (s)
White pine	30	0.09	41.8	10.0	33.3	54.5
"	"	0.14	2.3	0.3	2.0	2.5
"	"	0.18	1.1	0.1	1.0	1.3
"	60	0.07	16.6	7.5	10.0	24.8
"	"	0.09	16.8	7.3	11.1	25.0
"	"	0.14	5.3	4.7	1.3	11.6
"	"	0.18	2.6	2.5	1.0	6.3
PMMA	30	0.07	143.9	29.9	91.3	161.8
"	"	0.09	102.3	16.5	83.3	113.3
"	"	0.14	31.0	14.2	20	47
"	"	0.18	6.1	3.2	3.0	10.8
"	60	0.09	29.4	6.7	23.8	36.8
"	"	0.14	13.6	5.2	8.0	18.3
"	"	0.18	7.6	1.0	6.5	8.5

Table A-2. Experimental data set for 52 μm micronozzle array

Sample	Nozzle distance (cm)	Water flow (cm^3/s)	t_{ext} (s)	\pm SD (s)	$t_{\text{ext, min}}$ (s)	$t_{\text{ext, max}}$ (s)	N_2 co-flow
PMMA	40	0.11	74.2	11.2	61.3	80.8	No
"	"	0.17	57.9	7.5	50.0	65.0	No
"	"	0.20	7.4	2.1	5.0	8.8	No
"	40	0.11	7.0	3.7	4.8	11.3	Yes
"	"	0.17	6.5	6.5	2.5	14.0	Yes
"	"	0.20	1.1	0.4	0.8	1.5	Yes
"	50	0.11	61.5	34.3	37.3	85.8	No
"	"	0.17	59.3	18.4	46.3	72.3	No
"	"	0.20	50.0	3.5	47.5	52.5	No
"	50	0.11	7.5	5.0	4.3	13.3	Yes
"	"	0.17	4.2	3.6	1.8	8.3	Yes
"	"	0.20	3.7	0.4	3.3	4.0	Yes
"	60	0.11	98.6	13.3	89.3	108.0	No
"	"	0.17	61.3	4.6	58.0	64.5	No
"	"	0.20	34.8	9.6	28.0	41.5	No
"	60	0.11	9.5	10.7	2.5	21.8	Yes
"	"	0.17	23.5	10.2	14.3	34.5	Yes
"	"	0.20	2.5	0.9	2.0	3.5	Yes

Appendix B

Tables B-1 and B-2 tabulate all the experimental data obtained by using the piezoelectric droplet generator with a glass nozzle. In Table B-1, the data were taken with horizontal samples at two different nozzle-to-sample surface locations and with an external radiative heat flux of 25 kW/m². The data taken with inclined samples are listed in Table B-2. In the tables, t_{ext} is the average extinguishment time, SD is the standard deviation, $t_{ext, min}$ is the minimum extinguishment time observed, and $t_{ext, max}$ is the maximum extinguishment time observed.

Table B-1. Experimental data set for piezoelectric droplet generator (horizontal samples)

Sample	Nozzle distance (cm)	Water flow (cm ³ /s)	t_{ext} (s)	\pm SD (s)	$t_{ext, min}$ (s)	$t_{ext, max}$ (s)
PMMA	50	0.42	15.7	0.3	15.5	15.8
"	"	0.87	7.8	2.7	4.7	9.6
"	"	1.17	5.4	2.1	3.7	7.7
"	"	1.43	3.2	1.5	1.5	4.6
"	"	1.62	3.8	1.8	2.5	5.1
"	"	1.80	0.8	1.0	0.2	1.9
White pine	50	0.42	2.9	0.7	2.2	3.5
"	"	0.87	0.1	0.0	0.1	0.1
"	"	1.17	0.1	0.0	0.1	0.1
"	"	1.43	0.1	0.0	0.1	0.1
PS foam	50	0.42	25.0	2.9	23.0	27.0
"	"	0.87	9.8	0.5	9.5	10.1
"	"	1.17	3.3	2.6	1.5	6.3
"	"	1.43	1.6	0.2	1.4	1.7
"	"	1.62	1.1	0.1	1.0	1.2

Table B-1 (continued). Experimental data set for piezoelectric droplet generator (horizontal samples)

Sample	Nozzle distance (cm)	Water flow (cm ³ /s)	t_{ex} (s)	\pm SD (s)	$t_{ex, min}$ (s)	$t_{ex, max}$ (s)
PMMA	60	0.42	6.0	4.6	2.1	11.1
"	"	0.87	1.3	1.7	0.3	3.2
"	"	1.17	0.3	0.2	0.2	0.6
"	"	1.43	1.2	0.8	0.2	1.7
White pine	60	0.42	1.1	0.5	0.5	1.5
"	"	0.87	0.3	0.3	0.1	0.6
"	"	1.17	0.1	0.0	0.1	0.1
"	"	1.43	0.2	0.2	0.1	0.4
PS foam	60	0.42	8.1	3.1	4.7	10.9
"	"	0.87	1.6	0.5	1.1	2.1
"	"	1.17	2.5	1.8	1.1	4.6
"	"	1.43	1.2	0.1	1.1	1.3
"	"	1.62	1.1	0.2	0.9	1.3

Table B-2. Experimental data set for piezoelectric droplet generator (inclined samples)

Sample	Nozzle distance (cm)	Water flow (cm ³ /s)	t_{ext} (s)	\pm SD (s)	$t_{ext, min}$ (s)	$t_{ext, max}$ (s)
PMMA	50	0.42	3.4	1.1	2.6	4.7
"	"	0.87	4.5	3.3	2.4	8.3
"	"	1.17	4.1	1.0	3.2	5.1
"	"	1.43	3.7	0.2	3.5	3.9
"	"	1.62	3.4	1.0	2.7	4.6
White pine	50	0.42	3.8	1.1	2.6	4.7
"	"	0.87	3.9	1.0	3.0	5.0
"	"	1.17	0.7	1.0	0.1	1.9
"	"	1.43	1.1	1.0	0.3	2.2
"	"	1.62	2.1	0.8	1.1	2.6
PMMA	60	0.42	4.6	2.1	1.4	6.8
"	"	0.87	3.1	2.3	0.9	6.7
"	"	1.17	3.8	0.4	3.4	4.3
"	"	1.43	4.4	1.8	2.7	6.7
"	"	1.62	4.4	1.2	3.2	5.9
"	"	1.80	4.3	2.0	2.0	5.6
White pine	60	0.42	2.3	1.5	1.1	4
"	"	0.87	1.1	0.6	0.4	1.6
"	"	1.17	1.9	0.9	0.9	2.8
"	"	1.43	1.4	1.6	0.5	3.3
"	"	1.62	0.8	0.8	0.2	1.8

Appendix C

This appendix documents the cold-flow testing of a commercial low pressure, high momentum pendant water mist nozzle. The work constitutes a part of the overall water mist project funded by FEMA. The evaluation was conducted by Mr. Anthony D. Putorti, Mrs. Tamra D. Belsinger, and William H. Twilley under the direction of Mr. Daniel Madrzykowski of the Fire Safety Engineering Division of BFRL/NIST.

U.S. DEPARTMENT OF COMMERCE
NATIONAL INSTITUTE OF STANDARDS AND TECHNOLOGY
Gaithersburg, MD 20899

REPORT OF TEST
FR 4000

May 31, 1995

**Determination of Water Spray Drop Size and Velocity from a Low Pressure,
High Momentum, Water Mist Nozzle**

A.D. Putorti Jr., T.D. Belsinger, and W.H. Twilley
Building and Fire Research Laboratory
National Institute of Standards and Technology
U.S. Department of Commerce
Gaithersburg, MD 20899

Abstract

In order to characterize the water spray from a low pressure, high momentum water mist nozzle, measurements were made using an optical array probe droplet analyzer. The water droplet sizes and velocities from the nozzle were measured at varying operating conditions and locations in the spray field. The study resulted in droplet size and velocity ranges for the nozzle, as well as mean droplet velocities and droplet size distributions. The pendant nozzle used in this study is currently being evaluated by listing organizations for fire suppression in residential and light hazard occupancies.

DETERMINATION OF WATER SPRAY DROP SIZE AND VELOCITY FROM A LOW PRESSURE, HIGH MOMENTUM, WATER MIST NOZZLE

Anthony D. Putorti, Jr., Tamra D. Belsinger, and William H. Twilley
Building and Fire Research Laboratory

Introduction

The United States Fire Administration is currently investigating methods of lowering the costs of water-based fire suppression systems for use in residential occupancies. One possible method of reducing costs is to reduce the water demand of the suppression system by employing water mist nozzles. Water mist fire suppression systems have been shown to effectively control some types of fires, but have not, as of yet, been approved for use in residential occupancies.

As part of its water mist investigation, the Fire Administration has funded NIST to measure the droplet size range of the water mist produced by a pendant water mist nozzle. The nozzle under study is currently being evaluated by listing organizations for fire suppression systems in residential and light hazard occupancies.

In this study, the droplet size distribution from a water mist nozzle was measured at twenty-nine positions within the water mist pattern. Droplet size and velocity ranges were determined, and mean droplet velocities were calculated.

Droplet Analyzer

The size and velocity measurements were made using a self-contained laser probe operating on the shadowing principle. A laser beam passes from the laser, through the measuring volume, and onto a diode array. Particles passing through the measuring volume form a shadow on the diode array, which is detected by the probe. An image is formed by the probe, with the width of the line diode array forming one dimension, and the scanning of the array (time) forming the second dimension of the droplet image. A personal computer and control/data acquisition software record the sizes of individual droplets and information that can be used to calculate droplet velocity.

The probe electronics and software contain error correction and droplet verification routines which reject multiple droplets in the measuring volume, and droplets that are not completely within the measuring volume. The probe is capable of measuring droplets with diameters from 30 μm to 1860 μm , as configured by the manufacturer.

Experimental Configuration

The experiments were conducted in the NIST Large Fire Research Facility. The pendant style nozzle was mounted in the center of a nominally 2.44 m (8 ft) by 2.44 m (8 ft) smooth, flat, horizontal plywood ceiling, which was suspended inside an alcove measuring approximately 4.6 m (15 ft) by 6.0 m (20 ft) by 3.0 m (10 ft) high. A plan view of the alcove is shown in Figure C-1. The plywood ceiling was located $2.44 \text{ m} \pm 0.03 \text{ m}$ ($8.0 \text{ ft} \pm 0.1 \text{ ft}$) above the concrete floor of the alcove. In its mounted position, the deflector of the nozzle was located $0.030 \text{ m} \pm 0.005 \text{ m}$ from the ceiling. The ceiling

around the sprinkler was marked to indicate angular positions about the centerline of the nozzle, which acted as the origin. The markings allowed for repeatable rotation of the nozzle in its threaded fitting.

The droplet probe was mounted to the top of a cart equipped with a hydraulic lifting mechanism, allowing for adjustments in elevation. The cart travels on a straight track, limiting movement to a straight line, and reducing possible positioning errors. The elevation of the center of the measuring volume of the droplet probe was $1.50 \text{ m} \pm 0.02 \text{ m}$ below the nozzle deflector for all of the measurements. This distance was chosen as representative of the distance between a nominal 2.44 m (8.0 ft) ceiling and typical residential fuels such as beds and other types of furniture.

The water was supplied to the nozzle from the building water supply via one inch steel pipe. A ball valve and gate valve were used to turn the water on and off and to control the flow. A pressure gauge approximately 0.35 m (1.1 ft) above the nozzle was used to monitor water flow conditions. Figure C-2 shows a schematic of the experimental configuration.

In regards to the functioning of the water mist nozzle, the spray pattern of this particular nozzle demonstrated a tendency to be seriously affected by water-borne debris. Several times during the experiments, the spray pattern would suddenly undergo a very significant change, with an apparent loss of coverage area, spray momentum, and water flow rate. Upon removal and inspection of the nozzle, small amounts of rust and scale had lodged in the screen of the nozzle. Even though the quantity of debris was small, and blocked a small percentage of the screen, the spray pattern was drastically affected. In order to prevent clogging during the experiments discussed in this report, the piping was flushed daily, and the nozzle cleaned prior to the measurements.

Experiments

The construction of the water mist nozzle was radially symmetrical about two perpendicular axes. The sizes and velocities of the droplets produced by the nozzle were measured in various locations within one 90 degree sector of the water spray pattern, reflecting the observed symmetry in the water spray pattern.

Movement of the probe was limited to a straight line, therefore the nozzle was rotated in increments of 15 degrees. In order to compare measurements at different pressures, which cause changes in the shape of the nozzle spray envelope, the sampling locations were non-dimensionalized by the distance from the nozzle centerline to the edge of the spray envelope. The outermost measurement point for each pressure was made at the edge of the spray envelope for that pressure. The edge of the spray envelope was determined visually.

The flow rate corresponding to water pressure was measured by collecting and determining the mass of the discharged water over time. The nozzle was operated at $621 \text{ kPa} \pm 14 \text{ kPa}$ ($90.0 \text{ psi} \pm 2.0 \text{ psi}$) and $448 \text{ kPa} \pm 14 \text{ kPa}$ ($65.0 \text{ psi} \pm 2.0 \text{ psi}$), which resulted in flow rates of $186 \text{ cm}^3/\text{s} \pm 1 \text{ cm}^3/\text{s}$ ($2.948 \text{ gpm} \pm 0.016 \text{ gpm}$) and $158 \text{ cm}^3/\text{s} \pm 1 \text{ cm}^3/\text{s}$ ($2.507 \text{ gpm} \pm 0.016 \text{ gpm}$) respectively.

Figure C-3 shows the measurement locations, which are identified by an angle and a radial distance from the nozzle centerline. Table C-1 lists the radial distances for the two pressures that correspond to the positions in Figure C-3. The 0 degree positions are defined as perpendicular to the plane containing the nozzle arms. The standard uncertainty in the distance measurements in Figure C-3 is $\pm 0.01 \text{ m}$ ($\pm 0.03 \text{ ft}$), and ± 2 degrees.

The droplet size and velocity measurements were based on a minimum of 25000 verified drops for most of the experiments. In some cases, the droplet measurement rate was very low, due to the small number of drops reaching the outer edge of the water spray envelope. In some of these low data rate cases, 25000 verified drops were not measured, but sampling was conducted for a minimum of 600 s.

Results

The droplet size distribution for the water spray was measured at the twenty-nine locations shown in Figure C-3. The droplet size distributions for the experiments are shown in Tables C-2a and C-2b for the experiments conducted at $621 \text{ kPa} \pm 14 \text{ kPa}$ ($90.0 \text{ psi} \pm 2.0 \text{ psi}$), and Tables C-3a and C-3b for the experiments conducted at $448 \text{ kPa} \pm 14 \text{ kPa}$ ($65.0 \text{ psi} \pm 2.0 \text{ psi}$). The droplet diameters from the experiments were found to range from less than $36 \text{ }\mu\text{m}$ to $1230 \text{ }\mu\text{m}$ for the experiments conducted at $448 \text{ kPa} \pm 14 \text{ kPa}$ ($65.0 \text{ psi} \pm 2.0 \text{ psi}$), and range from less than $36 \text{ }\mu\text{m}$ to $1155 \text{ }\mu\text{m}$ for the experiments conducted at $621 \text{ kPa} \pm 14 \text{ kPa}$ ($90.0 \text{ psi} \pm 2.0 \text{ psi}$). The droplet diameter range represents 99.9 percent of the droplets measured; that is 0.1 percent of the droplets had diameters greater than the maximum stated value. The 99.9 percent criterion was used to eliminate the possibility of a small number of very large droplets skewing the droplet size range.

The standard uncertainty in the droplet size measurements is $\pm 15 \text{ }\mu\text{m}$. The repeatability of successive experiments over several days in the same sampling location was evaluated by the use of one standard deviation of the mean droplet size of identical experiments, resulting in a value of $25 \text{ }\mu\text{m}$ for the $448 \text{ kPa} \pm 14 \text{ kPa}$ ($65.0 \text{ psi} \pm 2.0 \text{ psi}$) experiments and $12 \text{ }\mu\text{m}$ for the experiments conducted at $621 \text{ kPa} \pm 14 \text{ kPa}$ ($90.0 \text{ psi} \pm 2.0 \text{ psi}$).

The velocities of the water droplets were calculated based on the time required for each individual drop to pass through the probe image field. The range of droplet velocities was found to be approximately 0.19 m/s to 1.58 m/s (0.62 ft/s to 5.18 ft/s), with a mean droplet velocity of approximately 0.58 m/s (1.90 ft/s), calculated from the experiments conducted at $448 \text{ kPa} \pm 14 \text{ kPa}$ ($65.0 \text{ psi} \pm 2.0 \text{ psi}$). For the measurements taken at $621 \text{ kPa} \pm 14 \text{ kPa}$ ($90.0 \text{ psi} \pm 2.0 \text{ psi}$), the droplet velocities ranged from approximately 0.25 m/s to 1.9 m/s (0.82 ft/s to 6.23 ft/s), with a mean droplet velocity of approximately 0.61 m/s (2.00 ft/s).

Table C-1. Radial position as a function of pressure

Location	Radial distance (m), (ft)	
	Low pressure experiments (448 ± 14) kPa (65.0 ± 2.0) psi	High pressure experiments (621 ± 14) kPa (90.0 ± 2.0) psi
A	0.00 (0.00)	0.00 (0.00)
B	0.34 (1.12)	0.29 (0.95)
C	0.68 (2.23)	0.58 (1.90)
D	1.01 (3.31)	0.87 (2.85)
E	1.35 (4.43)	1.17 (3.84)

Table C-2a. Droplet size distribution for 0-45 degrees at 621 kPa (90 psi)

Droplet size (μm)	Measurement position, angle																	
	A, 0	B, 0	C, 0	D, 0	E, 0	B, 15	C, 15	D, 15	E, 15	B, 30	C, 30	D, 30	E, 30	A, 45	B, 45	C, 45	D, 45	E, 45
36	9217	9754	7251	3877	2780	9244	8107	8751	3248	8764	10215	16277	14588	8487	9089	6089	3715	1302
66	4184	4413	3649	2135	1252	4529	4246	4186	1178	4184	5344	6672	7436	4271	4571	3638	1963	411
96	2453	2600	2236	1663	1001	3089	3097	2355	324	2561	3485	1919	2154	2957	2874	2857	1363	87
125	2165	1958	1896	1456	1113	2377	2459	1582	92	2010	2270	684	379	2636	2246	2508	1068	29
155	2288	1634	1873	1546	1371	2302	2163	1213	49	1960	1610	289	53	2772	2138	2655	928	8
185	2430	1493	1921	1761	1283	2006	1659	991	12	1786	1034	151	6	2706	1844	2538	741	12
214	2105	1343	1659	1497	1083	1661	1452	717	17	1611	721	95	1	2593	1522	2371	571	7
243	1603	1339	1629	1596	1005	1445	1368	663	6	1516	558	49	2	2032	1324	2444	543	10
273	909	884	1487	1733	846	813	1327	660	5	922	404	43	1	1022	889	2084	611	10
303	415	389	1085	1632	661	346	914	589	6	394	303	60	1	434	428	1401	741	4
332	152	174	763	1637	561	113	517	641	2	155	157	119	21	216	143	891	1299	3
362	70	65	447	1566	534	40	265	652	1	86	65	79	95	90	74	441	2055	3
391	26	29	261	1368	589	19	217	648	14	29	42	28	131	29	34	282	2356	3
421	16	14	174	1093	750	14	147	620	18	17	28	20	44	26	16	183	2184	13
450	10	7	110	817	898	10	100	504	30	7	9	44	17	11	16	117	1820	33
480	6	1	83	626	984	3	69	410	39	3	8	59	7	6	5	57	1269	51
510	4	2	60	456	1035	1	42	312	52	6	10	39	0	5	2	45	835	88
540	2	1	33	331	979	0	27	257	40	1	4	23	3	8	0	23	594	112
570	2	0	20	262	954	0	9	175	40	2	2	14	1	1	1	10	393	100
600	3	0	14	197	865	0	14	128	29	0	2	14	3	1	1	4	268	79
630	2	0	3	139	811	0	11	109	34	0	0	4	0	1	0	7	156	56
660	0	0	6	86	710	0	3	65	20	1	0	4	0	0	0	6	89	43
690	0	0	2	50	600	0	3	43	20	0	0	1	0	3	0	4	70	34
720	1	0	1	41	568	0	3	23	15	0	0	0	0	0	0	2	53	22
750	0	0	0	43	486	0	0	20	12	0	0	2	0	0	0	0	26	18
780	0	0	0	19	389	0	0	16	5	0	0	1	0	1	0	4	16	10
810	0	0	1	14	347	0	1	10	7	0	0	0	0	0	0	1	8	13
840	0	0	0	9	250	0	1	9	1	0	0	0	0	0	0	0	7	6
870	0	0	0	12	194	0	0	1	1	0	0	0	0	0	0	0	12	4
900-1860	0	0	0	13	632	0	0	5	6	0	0	1	0	0	0	0	9	11
Total	28063	26100	26664	27675	25531	28012	28221	26355	5323	26015	26271	26691	24943	30308	27217	30662	25763	2582

Table C-2b. Droplet size distribution for 60-90 degrees at 621 kPa (90 psi)

Droplet size (μm)	Measurement position, angle												
	B, 60	C, 60	D, 60	E, 60	B, 75	C, 75	D, 75	E, 75	A, 90	B, 90	C, 90	D, 90	E, 90
36	7651	7047	5500	3109	10220	10755	11108	13715	8756	10422	11654	19568	930
66	3589	3084	3052	1332	4637	5175	5374	6749	4430	5003	5758	9619	372
96	2597	2118	2535	1028	3014	3329	4190	2871	2886	3140	3467	5505	82
125	2135	1860	2239	860	2289	2245	1887	1019	2492	2106	2186	2682	23
155	2219	1901	2318	926	1942	1721	1104	323	2554	1724	1563	1421	7
185	1992	1963	2230	881	1494	1303	704	106	2563	1330	1001	711	1
214	1974	1766	2150	738	1435	1027	481	25	2266	1296	714	387	1
243	1781	1659	2220	752	1342	882	338	16	1643	1216	654	255	0
273	1257	1513	2232	590	859	687	285	7	912	740	714	210	0
303	569	1129	2008	482	371	462	207	8	390	287	425	306	0
332	231	694	1796	439	168	343	201	6	188	80	159	281	0
362	122	371	1522	399	55	195	181	34	79	24	54	89	1
391	38	245	1058	487	15	81	127	46	38	10	14	32	1
421	17	140	825	644	10	42	134	26	13	9	8	8	0
450	9	85	618	894	4	25	127	12	13	2	3	6	0
480	6	63	500	1165	3	14	126	19	4	0	1	3	0
510	2	40	292	1287	0	11	99	28	4	0	2	4	0
540	1	29	229	1237	1	3	65	25	4	0	0	0	0
570	1	9	138	1281	0	3	53	32	5	0	0	0	0
600	1	6	86	1194	0	0	25	27	0	0	0	0	0
630	0	6	70	1072	0	0	8	12	2	0	0	0	0
660	0	5	46	928	0	0	6	9	2	0	0	0	0
690	0	3	30	772	0	0	6	6	0	0	0	0	0
720	0	4	17	622	0	0	0	5	2	0	0	0	0
750	0	2	21	578	0	1	0	4	1	0	0	0	0
780	0	0	13	436	0	0	1	1	0	0	0	0	0
810	0	0	7	399	0	0	0	0	0	0	0	1	0
840	0	0	4	323	0	0	0	0	0	0	0	0	0
870	0	1	4	248	0	0	0	0	1	0	0	0	0
900-1860	0	0	8	729	0	0	0	0	1	0	0	0	0
Total	26192	25743	33768	25832	27859	28304	26837	25131	29249	27389	28377	41088	1418

Table C-3a. Droplet size distribution for 0-45 degrees at 448 kPa (65 psi)

Droplet Size (μm)	Measurement Position, Angle																	
	A, 0	B, 0	C, 0	D, 0	E, 0	B, 15	C, 15	D, 15	E, 15	B, 30	C, 30	D, 30	E, 30	A, 45	B, 45	C, 45	D, 45	E, 45
36	8759	7590	6098	5368	4614	4825	5879	6334	2416	9567	9571	906	426	6774	8117	8000	10008	373
66	4362	4358	3865	3250	2110	3124	3611	3831	1249	4634	5045	452	171	3786	4143	4441	5455	122
96	3416	3511	4080	2738	1808	2600	2706	2916	686	3179	4432	82	18	2972	3142	3459	3325	8
125	2785	2668	3310	2541	1654	2501	2661	2333	488	2403	2822	18	0	2909	2368	2668	2047	0
155	2685	2424	3017	2544	1489	2909	2805	2269	315	2191	1851	13	0	3167	2311	2377	1406	0
185	2201	2102	2352	2274	1130	3074	2624	2140	197	1780	1142	4	0	3097	2068	1928	848	0
214	1658	1763	2034	2032	1009	3005	2534	1670	106	1682	858	5	0	2692	1871	1575	552	0
243	1022	1545	1918	2016	835	2411	1867	1593	72	1416	707	1	0	1920	1602	1370	426	0
273	525	811	1500	1729	667	1305	1241	1321	52	843	623	4	0	936	1024	992	291	0
303	191	313	972	1354	480	588	702	967	48	303	522	4	0	416	412	637	272	0
332	79	138	550	1006	428	296	452	746	32	128	245	9	0	177	191	354	289	0
362	37	58	317	768	358	154	265	468	49	53	105	10	1	87	80	181	453	0
391	18	26	149	587	449	72	145	341	59	22	40	1	3	52	54	106	557	0
421	15	17	85	389	456	37	95	226	80	11	26	1	4	19	27	54	603	0
450	12	11	73	284	580	19	54	174	109	6	12	1	0	11	5	29	536	1
480	8	3	45	211	676	11	28	127	116	3	14	3	0	7	3	10	376	0
510	5	0	25	155	762	4	21	81	103	2	5	1	0	7	2	8	305	1
540	1	0	13	122	740	4	14	59	94	0	2	2	0	1	4	3	232	1
570	3	1	12	81	670	1	11	51	64	1	2	0	0	1	0	3	163	1
600	3	0	4	52	595	1	4	38	55	1	0	0	0	0	1	2	108	0
630	1	0	5	44	559	1	1	34	59	0	0	5	0	5	0	1	79	1
660	1	0	1	40	505	0	0	19	38	0	0	0	0	4	1	0	54	0
690	0	0	3	34	447	0	0	15	27	0	1	0	0	1	0	0	42	0
720	1	0	0	23	395	0	3	12	23	0	0	0	0	1	0	0	28	0
750	1	0	0	19	337	0	0	4	16	0	0	0	0	1	0	0	18	0
780	1	0	0	11	320	1	0	8	16	1	0	0	0	2	0	0	21	0
810	1	0	0	5	237	0	0	2	12	1	0	0	0	1	0	0	10	0
840	2	0	0	9	221	0	0	1	6	0	0	0	0	0	0	0	3	0
870	0	0	1	6	172	0	0	2	11	0	0	0	0	0	0	0	3	0
900-1860	0	0	0	11	660	1	0	4	33	1	1	0	0	3	1	0	7	1
Total	27793	27339	30429	29703	25363	26944	27723	27786	6631	28228	28026	1522	623	29048	27428	28198	28517	509

Table C-3b. Droplet size distribution for 60-90 degrees at 448 kPa (65 psi)

Droplet size (μm)	Measurement position, angle														
	B, 60	C, 60	D, 60	E, 60	B, 75	C, 75	D, 75	E, 75	A, 90	B, 90	C, 90	D, 90	E, 90		
36	7665	6867	2948	9807	9488	9485	9872	1484	6128	15355	7766	3043	332		
66	4023	3606	1631	316	4522	4782	5510	810	3268	8190	4243	1561	139		
96	3640	3049	1196	142	2872	2987	1704	297	2646	8177	4837	935	18		
125	2679	2465	1295	99	2122	2110	2184	71	2818	6616	3775	528	3		
155	2171	2470	1377	110	1915	1524	1599	14	3398	5661	2411	276	1		
185	1814	2130	1323	119	1628	1135	825	2	3487	4439	1542	114	0		
214	1559	2007	1238	89	1394	853	536	2	3260	3993	1037	42	1		
243	1597	1849	1422	103	1077	820	376	0	2486	3169	833	21	0		
273	957	1485	1510	86	549	827	295	2	1262	1547	817	16	0		
303	477	992	1518	65	247	658	220	1	576	604	520	33	0		
332	188	610	1552	45	92	381	305	1	261	208	184	78	0		
362	76	399	1599	43	37	223	373	2	126	90	63	54	5		
391	49	214	1461	37	15	172	275	14	53	39	23	27	2		
421	24	109	1355	21	5	103	182	16	27	14	17	10	1		
450	6	86	1108	38	0	64	218	7	17	4	7	2	0		
480	5	49	878	51	3	53	214	5	14	3	2	1	0		
510	2	33	752	77	1	39	238	0	4	2	0	0	0		
540	1	25	532	65	2	15	191	1	3	4	0	0	0		
570	1	14	434	101	0	12	152	2	5	0	0	0	0		
600	0	13	311	106	0	9	118	1	6	1	0	0	0		
630	0	9	274	93	0	3	97	1	3	0	0	0	0		
660	0	4	228	77	0	1	60	0	6	0	0	0	0		
690	0	3	180	79	0	2	49	1	2	0	0	0	0		
720	0	0	114	87	0	0	32	0	1	1	0	0	0		
750	0	0	77	82	0	0	30	1	2	0	0	0	0		
780	0	0	58	55	0	0	20	0	0	0	0	0	0		
810	0	0	46	50	0	0	18	0	0	0	0	0	0		
840	0	0	26	50	0	0	10	0	1	0	0	0	0		
870	0	0	23	37	0	0	7	0	0	0	0	0	0		
900-1860	0	0	48	134	0	0	12	0	7	0	0	0	0		
Total	26954	28678	26714	3477	26039	26228	27450	2755	29867	58337	28077	6741	502		

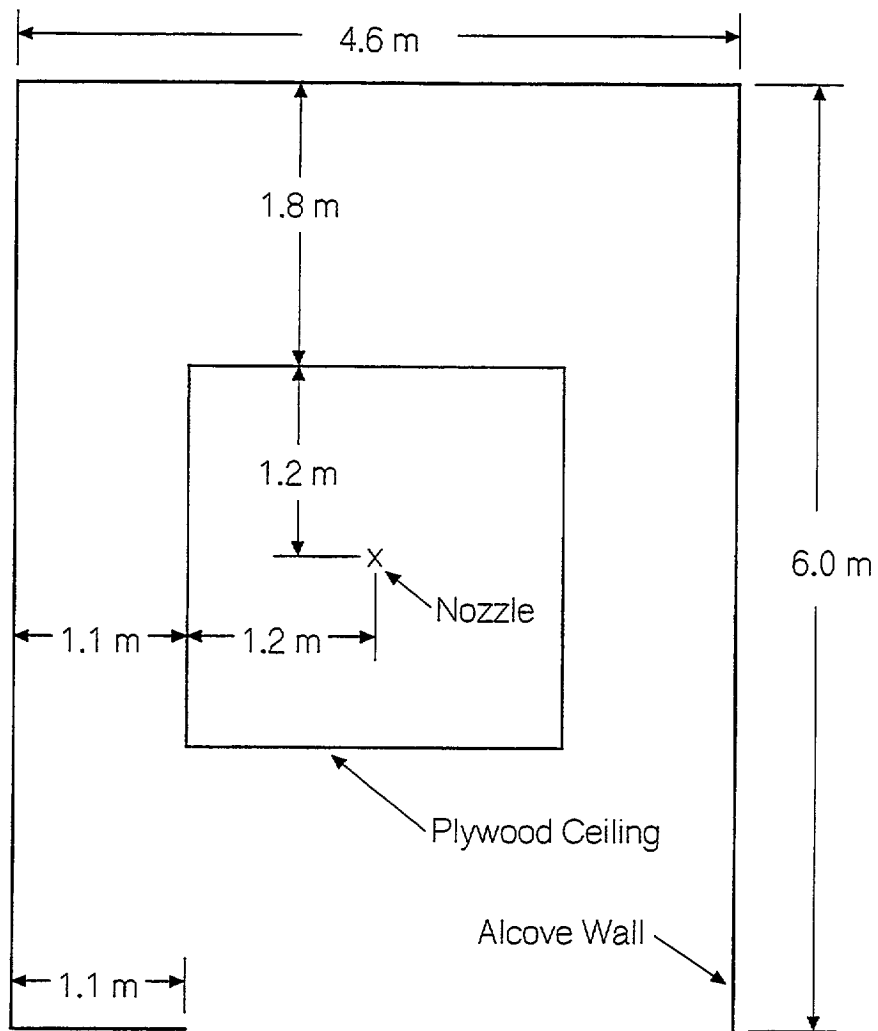


Figure C-1. Plan view of the nozzle alcove.

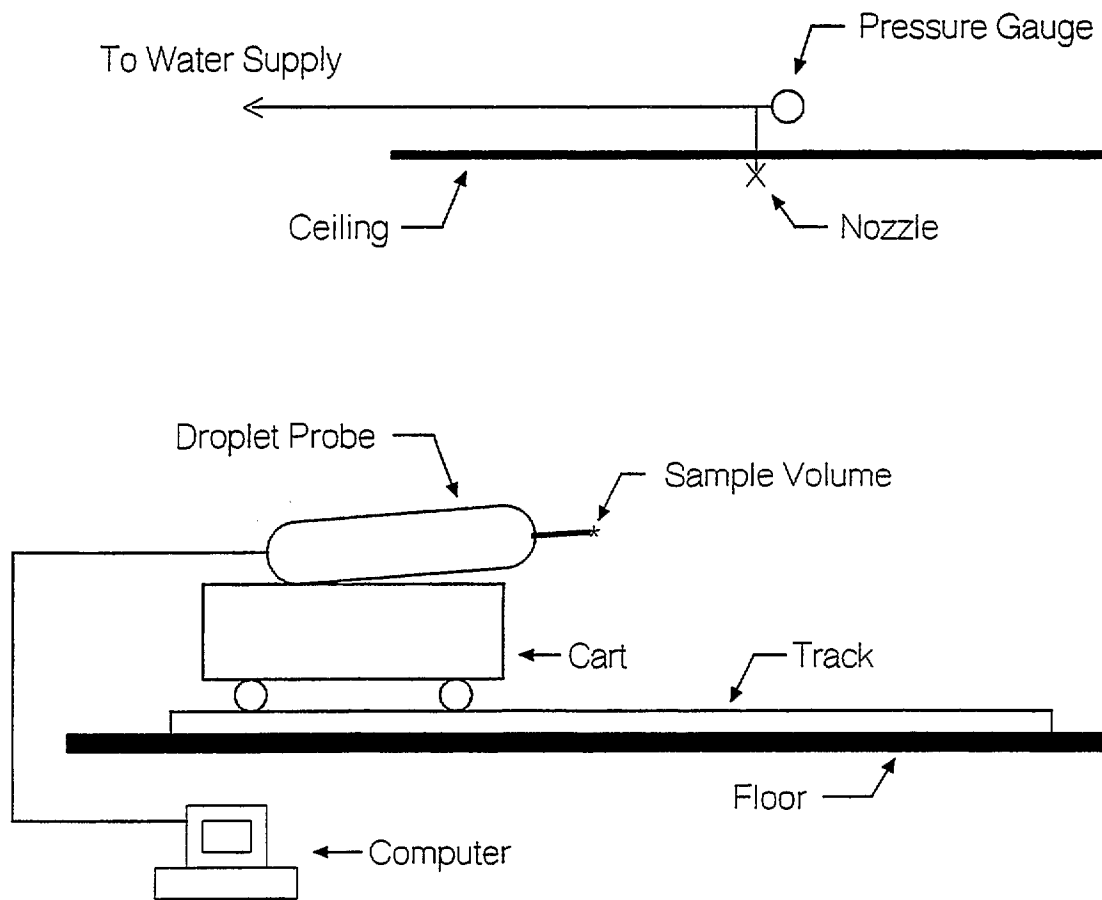


Figure C-2. Elevation view of the experimental configuration.

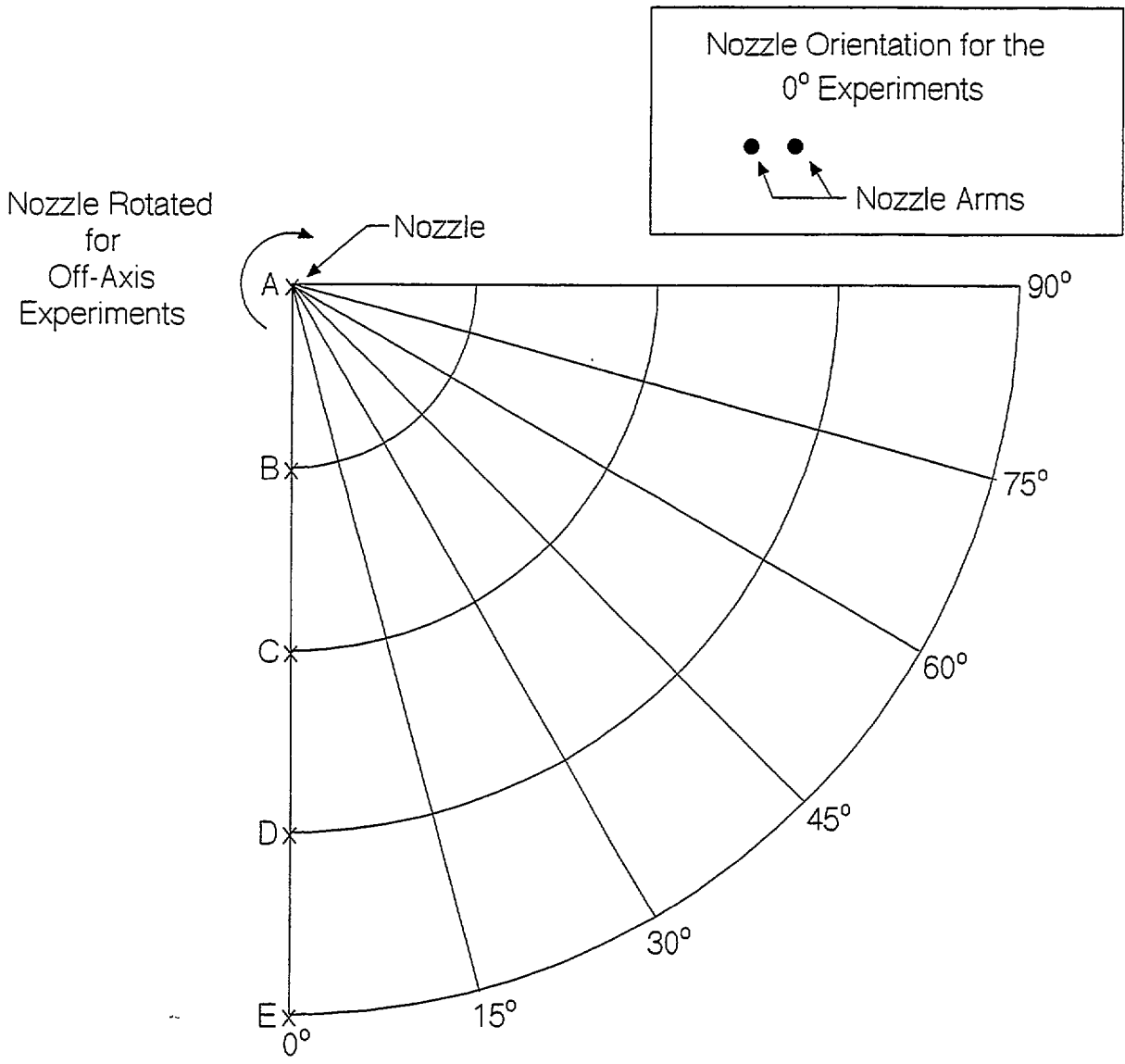
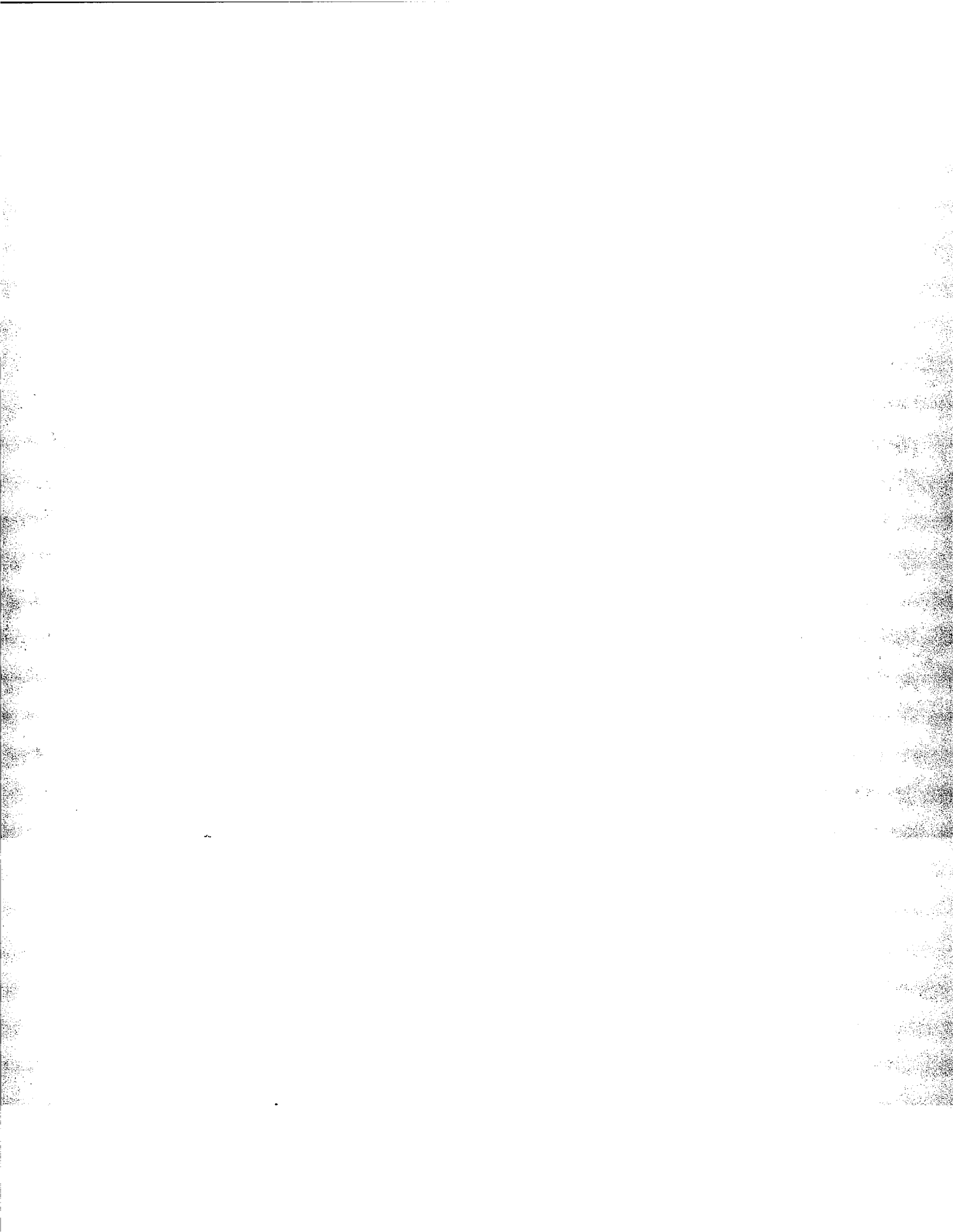


Figure C-3. Plan view of the measurement locations.



NIST-114 (REV. 6-93) ADMAN 4.09	U.S. DEPARTMENT OF COMMERCE NATIONAL INSTITUTE OF STANDARDS AND TECHNOLOGY	(ERB USE ONLY)	
MANUSCRIPT REVIEW AND APPROVAL		ERB CONTROL NUMBER	DIVISION
		PUBLICATION REPORT NUMBER NISTER 5795	CATEGORY CODE

INSTRUCTIONS: ATTACH ORIGINAL OF THIS FORM TO ONE (1) COPY OF MANUSCRIPT AND SEND TO THE SECRETARY, APPROPRIATE EDITORIAL REVIEW BOARD	PUBLICATION DATE April 1996	NUMBER PRINTED PAGES
--	--------------------------------	----------------------

TITLE AND SUBTITLE (CITE IN FULL)

Minimum Mass Flux Requirements to Suppress Burning Surfaces with Water Sprays

CONTRACT OR GRANT NUMBER	TYPE OF REPORT AND/OR PERIOD COVERED
--------------------------	--------------------------------------

AUTHOR(S) (LAST NAME, FIRST INITIAL, SECOND INITIAL) Yang, J.C., Boyer, C.I., and Grosshandler, W.L.	PERFORMING ORGANIZATION (CHECK (X) ONE BOX) <table style="width:100%; border-collapse: collapse;"> <tr> <td style="text-align: center;"><input checked="" type="checkbox"/></td> <td>NIST/GAITHERSBURG</td> </tr> <tr> <td style="text-align: center;"><input type="checkbox"/></td> <td>NIST/BOULDER</td> </tr> <tr> <td style="text-align: center;"><input type="checkbox"/></td> <td>JILA/BOULDER</td> </tr> </table>	<input checked="" type="checkbox"/>	NIST/GAITHERSBURG	<input type="checkbox"/>	NIST/BOULDER	<input type="checkbox"/>	JILA/BOULDER
<input checked="" type="checkbox"/>	NIST/GAITHERSBURG						
<input type="checkbox"/>	NIST/BOULDER						
<input type="checkbox"/>	JILA/BOULDER						

LABORATORY AND DIVISION NAMES (FIRST NIST AUTHOR ONLY)

BFRL/Fire Science Division 865

SPONSORING ORGANIZATION NAME AND COMPLETE ADDRESS (STREET, CITY, STATE, ZIP)

U.S. Fire Administration, Emmitsburg, MD 21721

PROPOSED FOR NIST PUBLICATION

<input type="checkbox"/> JOURNAL OF RESEARCH (NIST JRES) <input type="checkbox"/> J. PHYS. & CHEM. REF. DATA (JPCRD) <input type="checkbox"/> HANDBOOK (NIST HB) <input type="checkbox"/> SPECIAL PUBLICATION (NIST SP) <input type="checkbox"/> TECHNICAL NOTE (NIST TN)	<input type="checkbox"/> MONOGRAPH (NIST MN) <input type="checkbox"/> NATL. STD. REF. DATA SERIES (NIST NSRDS) <input type="checkbox"/> FEDERAL INF. PROCESS. STDS. (NIST FIPS) <input type="checkbox"/> LIST OF PUBLICATIONS (NIST LP) <input checked="" type="checkbox"/> NIST INTERAGENCY/INTERNAL REPORT (NISTIR)	<input type="checkbox"/> LETTER CIRCULAR <input type="checkbox"/> BUILDING SCIENCE SERIES <input type="checkbox"/> PRODUCT STANDARDS <input type="checkbox"/> OTHER _____
---	---	--

PROPOSED FOR NON-NIST PUBLICATION (CITE FULLY)	<input type="checkbox"/> U.S.	<input type="checkbox"/> FOREIGN	PUBLISHING MEDIUM <table style="width:100%; border-collapse: collapse;"> <tr> <td style="text-align: center;"><input checked="" type="checkbox"/></td> <td>PAPER</td> <td style="text-align: center;"><input type="checkbox"/></td> <td>CD-ROM</td> </tr> <tr> <td style="text-align: center;"><input type="checkbox"/></td> <td>DISKETTE (SPECIFY)</td> <td colspan="2"></td> </tr> <tr> <td style="text-align: center;"><input type="checkbox"/></td> <td>OTHER (SPECIFY)</td> <td colspan="2"></td> </tr> </table>	<input checked="" type="checkbox"/>	PAPER	<input type="checkbox"/>	CD-ROM	<input type="checkbox"/>	DISKETTE (SPECIFY)			<input type="checkbox"/>	OTHER (SPECIFY)		
<input checked="" type="checkbox"/>	PAPER	<input type="checkbox"/>	CD-ROM												
<input type="checkbox"/>	DISKETTE (SPECIFY)														
<input type="checkbox"/>	OTHER (SPECIFY)														

SUPPLEMENTARY NOTES

ABSTRACT (A 2000-CHARACTER OR LESS FACTUAL SUMMARY OF MOST SIGNIFICANT INFORMATION. IF DOCUMENT INCLUDES A SIGNIFICANT BIBLIOGRAPHY OR LITERATURE SURVEY, CITE IT HERE. SPELL OUT ACRONYMS ON FIRST REFERENCE.) (CONTINUE ON SEPARATE PAGE, IF NECESSARY.)

Experimental measurements of extinguishment times of burning solid fuels using water were conducted using a prototype micronozzle array and a piezoelectric droplet generator. Solid fuels considered included solid white pine, polymethyl methacrylate, and polystyrene foam. External heat flux was applied to the sample surface during burning. The effects of drop size, sample orientation with respect to the nozzle, and nozzle distance from the sample surface on extinguishment time were examined. The extinguishment time was found to decrease with increasing water flow rate. For a given water flow rate, significant reduction in extinguishment time was observed when smaller droplets were used. At low water flow rates, the extinguishment time decreased when the nozzle was positioned further from the sample surface. At high flow rates, the extinguishment was independent of the nozzle-to-sample distance. When the droplet stream was 45° relative to the sample, the extinguishment time was not affected by the nozzle-to-surface distance.

The other component of the project was to evaluate a commercial low pressure, high momentum pendent water mist nozzle using an optical array probe droplet analyzer. The pendent nozzle used in this study is currently being evaluated by listing organizations for fire suppression in residential and light hazard occupancies. The objective of this study was to determine drop size and velocity distributions at various locations in the spray. Experiments were conducted at 621 kPa ± 14 kPa (90.0 psi ± 2.0 psi) and 448 kPa ± 14 kPa (65.0 psi ± 2.0 psi). The droplet diameters from the experiments were found to range from less than 36 μm to 1230 μm for the experiments conducted at 448 kPa ± 14 kPa (65.0 psi ± 2.0 psi), and to range from less than 36 μm to 1155 μm for the experiments conducted at 621 kPa ± 14 kPa (90.0 psi ± 2.0 psi). The velocities of the water droplets were calculated based on the time required for each individual drop to pass through the probe image field. The range of droplet velocities was found to be approximately 0.19 m/s to 1.58 m/s (0.62 ft/s to 5.18 ft/s) from the experiments conducted at 448 kPa ± 14 kPa (65.0 psi ± 2.0 psi). For the measurements taken at 621 kPa ± 14 kPa (90.0 psi ± 2.0 psi), the droplet velocities ranged from approximately 0.25 m/s to 1.9 m/s (0.82 ft/s to 6.23 ft/s).

KEY WORDS (MAXIMUM OF 9; 28 CHARACTERS AND SPACES EACH; SEPARATE WITH SEMICOLONS; ALPHABETIC ORDER; CAPITALIZE ONLY PROPER NAMES)

Drop size measurements; extinguishment times; fire research; fire suppression; mist; sprays; polymethylmethacrylate; polystyrene foams; wood

AVAILABILITY

<input checked="" type="checkbox"/>	UNLIMITED	<input type="checkbox"/>	FOR OFFICIAL DISTRIBUTION - DO NOT RELEASE TO NTIS
<input type="checkbox"/>	ORDER FROM SUPERINTENDENT OF DOCUMENTS, U.S. GPO, WASHINGTON, DC 20402		
<input checked="" type="checkbox"/>	ORDER FROM NTIS, SPRINGFIELD, VA 22161		

NOTE TO AUTHOR(S): IF YOU DO NOT WISH THIS MANUSCRIPT ANNOUNCED BEFORE PUBLICATION, PLEASE CHECK HERE.

